The Campotosto linkage fault zone between the 2009 and 2016 seismic sequences of central Italy: Implications for seismic hazard analysis

Emanuele Tondi[1,2], Danica Jablonská[1], Tiziano Volatili[1], Maddalena Michele[2], Stefano Mazzoli[1], and Pietro Paolo Pierantoni[1,†]

[1]*School of Science and Technology, Geology Division, University of Camerino, Camerino, 62032 Macerata, Italy*
[2]*Istituto Nazionale di Geofisica e Vulcanologia, 00143 Rome, Italy*

ABSTRACT

In the last decade central Italy was struck by devastating seismic sequences resulting in hundreds of casualties (i.e., 2009-L'Aquila moment magnitude [Mw] = 6.3, and 2016-Amatrice-Visso-Norcia Mw max = 6.5). These seismic events were caused by two NW-SE–striking, SW-dipping, seismogenic normal faults that were modeled based on the available focal mechanisms and the seismic moment computed during the relative mainshocks. The seismogenic faults responsible for the 2009-L'Aquila Mw = 6.3 (Paganica Fault—PF) and 2016-Amatrice-Visso-Norcia Mw max = 6.5 (Monte Vettore Fault—MVF) are right-stepping with a negative overlap (i.e., underlap) located at the surface in the Campotosto area. This latter was affected by seismic swarms with magnitude ranging from 5.0 to 5.5 during the 2009 seismic sequence and then in 2017 (i.e., a few months later than the mainshocks related with the 2016 seismic sequence).

In this paper, the seismogenic faults related to the main seismic events that occurred in the Campotosto Seismic Zone (CSZ) were modeled and interpreted as a linkage fault zone between the PF and MVF interacting seismogenic faults. Based on the underlap dimension, the seismogenic potential of the CSZ is in the order of Mw = 6.0, even in the case that all the faults belonging to the zone were activated simultaneously. This has important implications for seismic hazard assessment in an area dominated by the occurrence of a major NW-SE–striking extensional structure, i.e., the Monte Gorzano Fault (MGF). Mainly due to its geomorphologic expression,
this fault has been considered as an active and silent structure (therefore representing a seismic gap) able to generate an earthquake of Mw max = 6.5–7.0. However, the geological evidence provided with this study suggests that the MGF is of early (i.e., pre- to syn-thrusting) origin. Therefore, the evaluation of the seismic hazard in the Campotosto area should not be based on the geometrical characteristics of the outcropping MGF. This also generates substantial issues with earthquake geological studies carried out prior to the recent seismic events in central Italy. More in general, the 4-D high-resolution image of a crustal volume hosting an active linkage zone between two large seismogenic structures provides new insights into the behavior of interacting faults in the incipient stages of connection.

INTRODUCTION

Central Italy was struck by severe earthquakes along the Apennine chain, as documented by historical sources (Rovida et al., 2019). The most significant earthquakes, clustering along the central Apennines fault system (CAFS; Cello et al., 1997), occurred in three periods over the last millennium: in the 13th-14th and the 17th-18th centuries, and then from the 1980's to the present (Tondi and Cello, 2003; Castelli et al., 2016; Rovida et al., 2019). The last decades witnessed several devastating earthquakes resulting in hundreds of casualties (i.e., 1997-Colfiorito-Sellano moment magnitude [Mw] = 6.0; 2009-L'Aquila Mw = 6.3; and 2016-Amatrice-Visso-Norcia Mw max = 6.5; Amato et al., 1998; Chiarabba et al., 2009; Chiaraluce et al., 2011; Chiaraluce et al., 2017. These events were caused by the reactivation of NW-SE–striking, SW-dipping normal faults (Tondi et al., 2009; Pantosti and Boncio, 2012; Pierantoni et al., 2013; Galli et al., 2017; Pizzi et al., 2017; Civico et al., 2018; Bignami et al., 2019; Villani et al., 2018) (Fig. 1).

The CAFS is an interactive active fault system, extending along the central Apennines in a north-south direction for a length of ∼100 km and ∼50 km of width (Cello et al., 1997). This system includes several active and capable faults (sensu IAEA, 2010), interpreted as the surface expression of deep seismogenic faults (Barchi et al., 2000; Galadini and Galli, 2000; Tondi, 2000). Many of the scientific papers on these active faults were published before the last destructive seismic sequences (in addition to those already mentioned, see also: Pizzi et al., 2002; Tondi and Cello, 2003; Galadini and Galli, 2003; Boncio et al., 2004a; Tondi et al., 2009). From 1997 to 2016, the entire fault system was activated along its length (see Fig. 1), thus providing the unique opportunity to evaluate the seismic hazard estimated by geological and paleoseismological studies. Furthermore, the latest seismic sequences have clearly demonstrated the dominant role of extensional tectonics in the upper crust of the central Apennines, with the main seismogenic sources dipping to the southwest (e.g., Galli et al., 2018; Galderisi and Galli, 2020).

A meaningful comparison may now be carried out considering the seismological data provided, in particular, by the 2009-L'Aquila (Mw = 6.3) and the 2016-Amatrice-Visso-Norcia (Mw max = 6.5) earthquakes. Moreover, these high-resolution data, together with the geological surveys carried out immediately after the mainshocks, allowed us to improve our knowledge on the seismotectonic setting of central Italy, and on both the peculiar phenomenology of earthquakes associated with crustal normal faults (Doglioni et al., 2015) and the interaction processes between active faults and earthquakes (Pino et al., 2019). Such interaction processes may be better understood considering the recent results on rupture directivity provided by Calderoni et al. (2017) for sixteen earthquakes of Mw > 4.4 belonging to the 2016 Amatrice-Norcia-Visso seismic sequences.

Pietro Paolo Pierantoni http://orcid.org/0000-0002-1237-4689

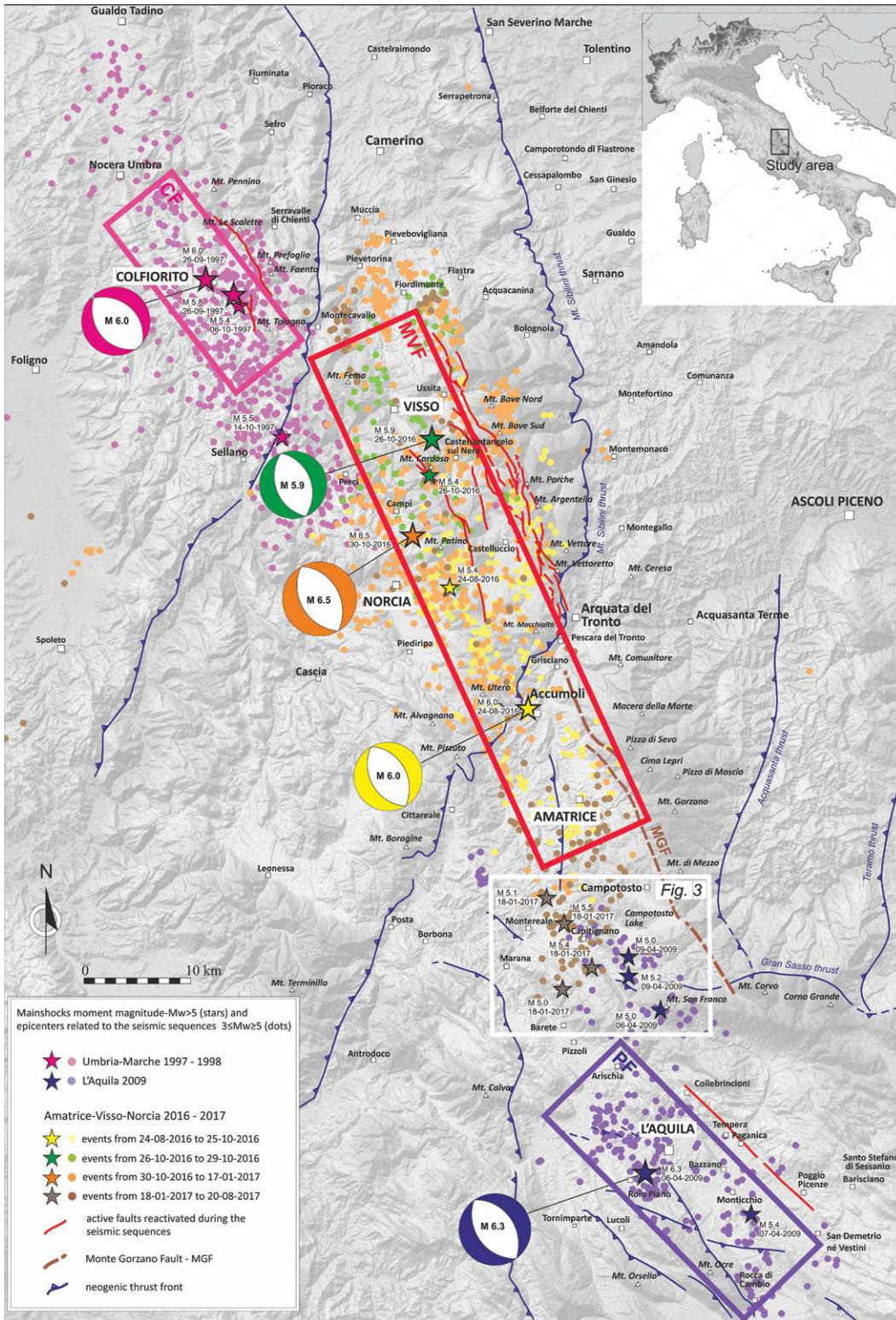†Corresponding author: pietropaolo.pierantoni@ unicam.it.

Figure 1. Map of the seismic sequences that took place in the last decades in central Italy. Focal mechanisms refer to the related mainshocks. Capable faults and modeled seismogenic faults are also shown (CF—Colfiorito Fault; MVF—Monte Vettore Fault; PF—Paganica Fault) (Tondi et al., 2009; Pantosti and Boncio, 2012, Pizzi et al., 2017; Chiarabba et al., 2018; Falcucci et al., 2018). The Campotosto area represented in Figure 3 is also shown.

The seismic sequences that occurred in the last decades in central Italy (Rovida et al., 2019; Chiaraluce et al., 2017) permit to: (a) verify the geological and paleoseismological analyses carried out prior to the seismic events, (b) improve our knowledge on the seismotectonic setting of central Italy, and (c) better understand the interaction processes between active faults (long-term) and earthquakes (shorth-term) within an active fault system (i.e., the CAFS in Cello et al., 1997; see also Calamita and Pizzi, 1992, 1994; Boncio et al., 2004a; Galadini, 1999; Galadini and Galli, 2000; Mildon et al., 2017; Wedmore et al., 2017).

Within the CAFS, the most recent seismic sequence of 2016 bridged the two former

epicentral areas of Colfiorito (in 1997) and L'Aquila (in 2009). A few days after the mainshock of L'Aquila (in 2009) and a few months after the mainshocks of Norcia (in 2016), seismic swarms with magnitudes ranging from 5.0 to 5.5 occurred in the Campotosto area, between the Paganica Fault (PF) and the Monte Vettore Fault (MVF) (Fig. 1). The occurrence of seismic swarms in the Campotosto area suggests a strong interaction between the seismogenic faults belonging to the CAFS (Cheloni et al., 2014; Calderoni et al., 2017; Mildon et al., 2017; Chiarabba et al., 2018; Pino et al., 2019), as already shown by the characteristics of the historical seismic sequences (e.g., multiple seismic events that occurred in 1703; Rovida et al., 2019) and by the spatial characteristics and the relationships of the dimensional parameters of the active faults along the Apennines (Cello et al., 1998a; Cowie and Roberts, 2001; Tondi and Cello, 2003; Spina et al., 2008, 2009; Mildon et al., 2017; Wedmore et al., 2017).

Fault interaction and fault-growth by segment linkage represent fundamental processes controlling the evolution, in both time and the space, of fault systems (Cartwright et al., 1995; Soliva et al., 2006; Fossen and Rotevatn, 2016, and references therein; Stemberk et al., 2019). Once two sub-parallel fault segments get close enough, they will start to interact. According to the spatial relationship between the two interacting faults, the interaction and relative linkage may encompass different processes and stages of evolution. Starting with a negative overlap geometry (i.e., underlap), if strain continues to be accommodated, a soft-linked stage (with a zone of subsidiary structures, represented by minor faults and fractures) and/or relay ramp formation (Walsh and Watterson, 1991) will

eventually result in a linkage of the two faults (hard-linkage).

The critical nearness or spacing between two fault tips interacting each other is of fundamental importance during the growth of fault populations. Mechanically, this critical spacing has been related to the zone of stress perturbation that occurs around faults (e.g., Ackermann and Schlische, 1997; Cowie and Roberts, 2001; Soliva et al., 2006; King and Deves, 2015). The effect of such stress perturbed regions has been explored by Willemse et al. (1996) and further by Gupta and Scholz (2000), whose modeling confirmed that tip propagation is enhanced or retarded as a fault grows into the stress increase or stress drop regions of an underlapping or overlapping fault, respectively (Fig. 2) (Scholz and Cowie, 1990; Marrett and Allmendinger, 1990; Peacock and Sanderson, 1991; Villemin et al., 1995; Schlische et al., 1996; Walsh et al., 2002; Wilkins and Gross, 2002; Soliva and Benedicto, 2004).

The type of interaction between faults and the rate at which faults reactivate not only control the long-term tectonic evolution of an area, but also influence seismic hazard, as earthquake recurrence intervals tend to decrease as fault slip rate increase (Roberts et al., 2004; Spina et al., 2008; Wedmore et al., 2017). Furthermore, short-term interaction may generate larger and/or multiple earthquakes (Stein et al., 1992, 1997; Spina et al., 2008, 2009).

In this paper, the seismogenic faults related to the main seismic events that occurred in the Campotosto area are first reconstructed based on seismological evidence. Subsequently, new geological data are presented. The seismological and geological data are then discussed within the framework of a new seismotectonic

scenario for the 2009-L'Aquila and 2016-Amatrice-Visso-Norcia seismic sequences. A critical reassessment of previous works is also carried out, particularly concerning the activity of the major NW-SE–striking extensional structure of the region, i.e., the Monte Gorzano Fault (MGF).

The MGF is a large structure that has been considered as a Quaternary, active, capable, and silent fault (i.e., representing a seismic gap), able to generate an earthquake of Mw max = 6.5–7.0 (Galadini and Galli, 2003; Boncio et al., 2004b; Falcucci et al., 2018 and reference therein). However, based on new field observations and building on previous studies and available data, we provide an alternative model implying an earlier evolution of the MGF. Moreover, in light of the outcomes provided by the seismic and geological data related to the earthquake sequences that occurred in the last decades in central Italy, we discuss relevant issues concerning earthquake geological studies carried out prior to the seismic events.

THE CAMPOTOSTO SEISMIC ZONE

The CSZ, located between the PF and MVF (Fig. 1), was affected by seismic swarms with maximum magnitude ranging from 5.0 to 5.5 (Fig. 3) during both the 2009-L'Aquila and 2016-Amatrice-Visso-Norcia seismic sequences (Valoroso et al., 2013; Chiaraluce et al., 2017). The CSZ hypocenters related with the 2009-L'Aquila seismic sequence show a depth distribution in the range of 5–12 km. The related focal mechanisms are all of a similar type (Fig. 3; Valoroso et al., 2013), consistent with the orientation of the ongoing extensional tectonic stress that affects the area (Mariucci et al., 2010; Mariucci and Montone 2016), and the
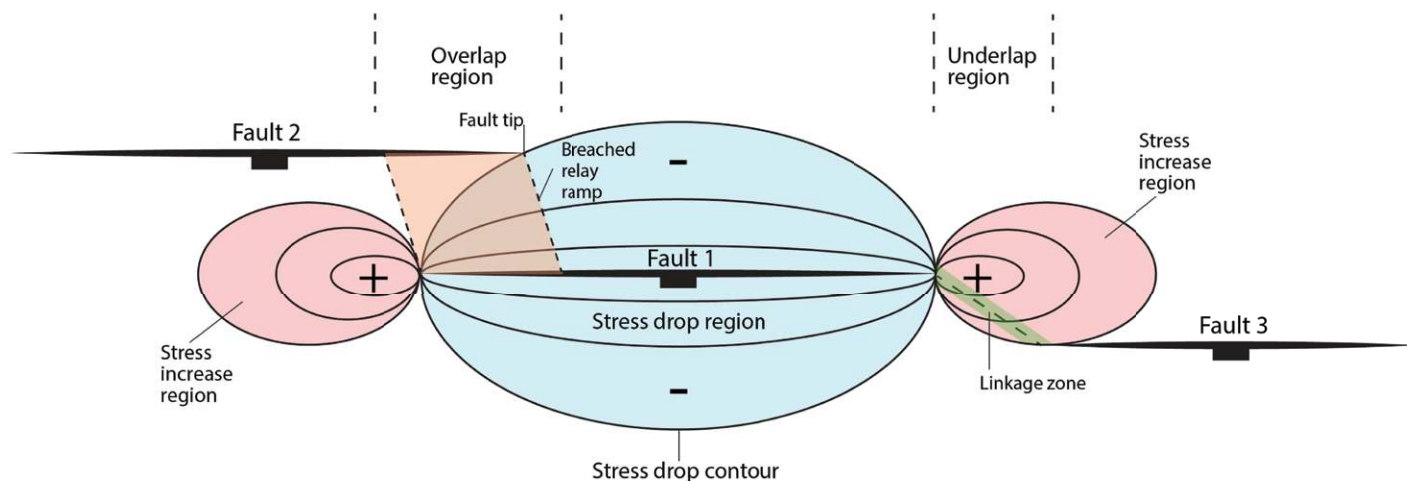

Figure 2. Different processes/stages of evolution of linkage between neighboring normal faults in relation to their geometry (modified after Gupta and Scholz, 2000). Fault 1 and Fault 3 display the geometrical relationship between the Paganica Fault (Fault 3) and the Monte Vettore Fault (Fault 1). The underlap region represents the Campotosto area, central Italy.
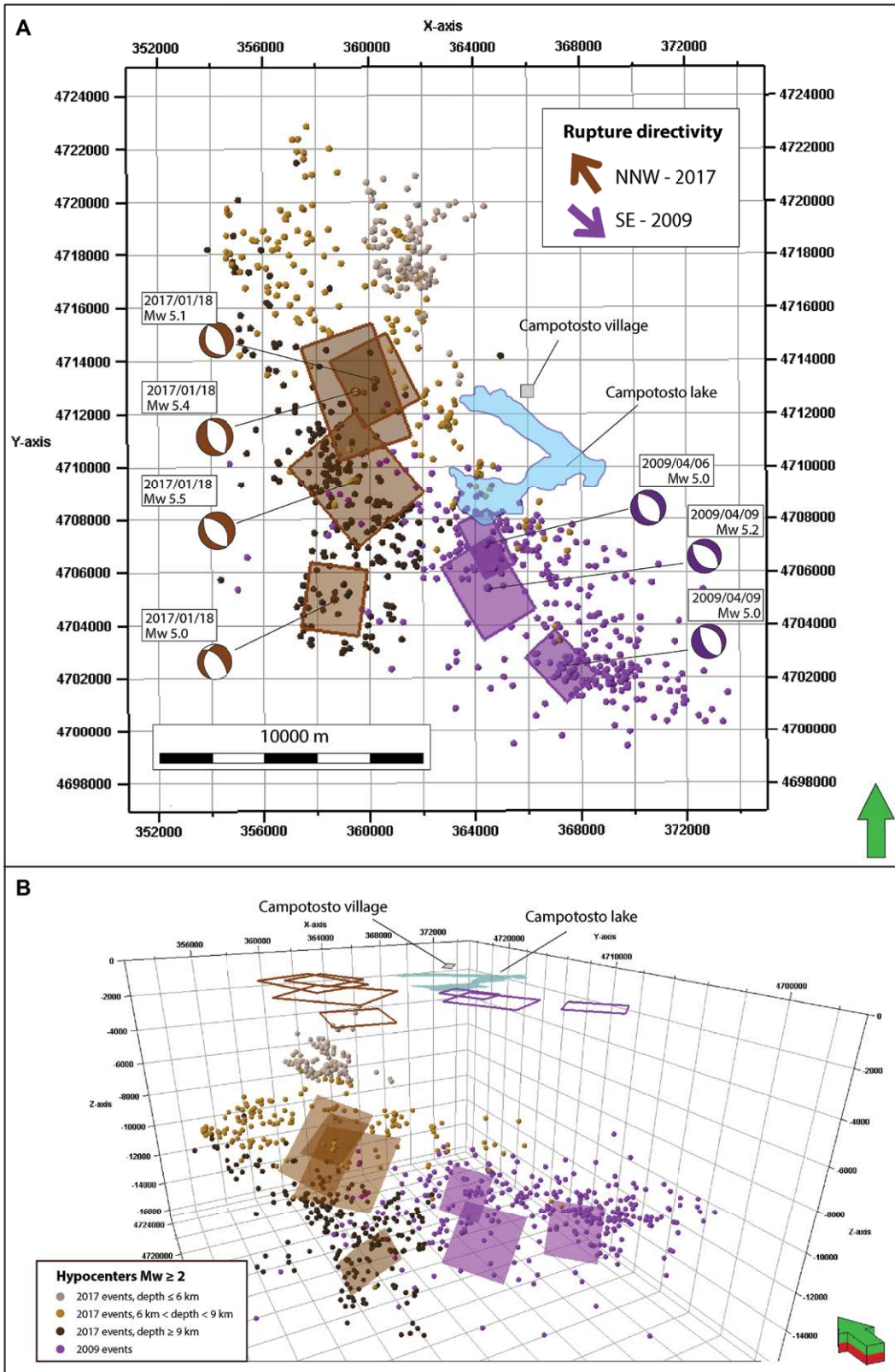
Figure 3. (A) Map view of the Campotosto Seismic Zone (CSZ), central Italy, showing epicenter distribution (moment magnitude [Mw] ≥ 2.0) of seismic events that took place within five days after each of the main events. Modeled seismogenic faults are displayed with the related focal mechanisms (http://cnt.rm.ingv.it/en/tdmt; Scognamiglio et al., 2006). Events associated with the two distinct seismic sequences are shown in different tonality of brown depending on hypocentral depth (January 2017) and in purple (April 2009). (B) 3-D representation of hypocenter distribution within the CSZ, enhancing the visualization of event clusters in depth and the geometry of the modeled fault planes. The information of rupture directivity is from Calderoni et al. (2017).

PF attitude and kinematics are compatible with them. On the other hand, during the 2016-Amatrice-Visso-Norcia seismic sequence, the main events within the CSZ show a more heterogeneous orientation of the nodal planes. These tend to cluster along two distinct, NNW and NW, trends (Fig. 3). The northern events, defining nodal planes alignments striking roughly in the same direction as the MVF, occur at a depth

in the range of 5–7 km. The southern events, approaching the 2009 CSZ events, are characterized by NS and NW trends and are deeper (in the range of 7–12 km).

The seismicity of the CSZ during the 2009-L′Aquila and 2016-Amatrice-Visso-Norcia seismic sequences was characterized by a total of seven mainshocks with magnitude ranging from 5.0 to 5.5, each followed by a coherent aftershock sequence. The three main events associated with the 2009-L′Aquila sequence and the four main events associated with the 2016-Amatrice-Visso-Norcia seismic sequence indicate the presence of a deep seismogenic source zone clearly interacting with both the PF and the MVF. It is important to note that the data provided by Calderoni et al. (2017) unravel the occurrence of two preferential rupture directivities for the 2009 and 2017 seismic events, in relation with the main seismogenic source with which they interact.

The Seismogenic Faults

To investigate the spatial and geometrical characteristics of the structures responsible for the mainshocks of the 1997, 2009, and 2016 seismic sequences, the seismogenic faults were modeled based on the seismological evidence (Fig. 1). Modeling followed the geometrical reconstruction available in the literature for the considered faults (Boncio et al., 2004a; Pizzi et al., 2017; Chiarabba et al., 2018; Falcucci et al., 2018; Walters et al., 2018), integrated and compared with the available focal mechanisms and the seismic moment detected during the following mainshocks (Fig. 1): (1) Colfiorito Fault—26 September 1997 Umbria-Marche earthquake (Mw = 6.0); (2) Paganica Fault (PF)—6 April 2009 L′Aquila earthquake (Mw = 6.3); (3) Monte Vettore Fault (MVF)—cumulative of 24 August 2016 Amatrice earthquake (Mw = 6.0), 26 October 2016 Visso

earthquake (Mw = 5.9), and 30 October 2016 Norcia earthquake (Mw = 6.5).

It is important to note that the MVF in Figure 1 represents the cumulative seismic ruptures of the three above-mentioned earthquakes and does not depict a single fault plane. Both seismological and geodetic (global positioning system [GPS], Differential Synthetic Aperture Radar Interferometry [DinSAR]) investigations following the 2016 seismic sequence highlighted an important segmentation of the MVF, with a major—active or passive—control exerted by pre-existing cross structures (e.g., Chiaraluce et al., 2017; Pizzi e al., 2017).

The seismogenic fault geometry of the main events (Mw ≥ 5.0) that occurred in the CSZ was modeled in 2-D and 3-D using the Petrel software (licensed for academic use by Schlumberger®) (Figs. 3A and 3B). Fault geometrical parameters including length (L) and area (A), and maximum coseismic displacement (D) for the seven main events affecting the CSZ are listed in Table 1. These parameters were estimated based on well-established relationships between seismic moment (Mo) (http://cnt.rm.ingv.it/en/tdmt; Scognamiglio et al., 2006), fault size, and D (Stein and Wysession, 2003; Zoback and Gorelick, 2012). For the 2009-L′Aquila seismic sequence, Calderoni et al. (2013) calculated a typical stress drop value of 10 MPa for earthquakes with Mw > 4.5. Taking into account the proximity of the two zones and their similarity from an active tectonics point of view, in this work we use the same stress drop value to estimate the maximum displacement D.

The applied workflow to reconstruct the seismogenic structures in Petrel involved the following: (a) the hypocenters, relocated using the Double-Difference technique (hypo-DD; Waldhauser and Ellsworth, 2000), were imported into the software as file ASCII with Universal Transverse Mercator coordinates; (b) from each hypocenter, a polygon was generated with the relative

fault dimension (Table 1); (c) these surfaces were then oriented in space according to the strike and dip angle of the relative focal mechanism; (d) finally, the seismogenic boxes (2-D projections of the seismogenic faults at the surface) were created assigning to the rectangles bounding the faults an elevation value (z) equal to 0.

The modeled seismogenic faults in the CSZ were assumed as having an aspect ratio (length/width) of 1, since we do not have any constraint on the shape of these structures. Fault attitude was obtained from the SW-dipping nodal planes, consistent with the distribution of the hypocenters (Mw > 2.0) that took place within a short time window (five days after the main event).

The modeled seismogenic sources (Fig. 3B) allow us to obtain a 3-D view of the seismogenic structures of the CSZ. This consists of fault planes not aligned along a preferential orientation and clearly represents an intensely fractured zone between the PF and MVF (see Fig. 3).

The Monte Gorzano Fault

The MGF, also known as Monti della Laga Fault, is a NW-SE–striking, SW-dipping normal fault. It is located in an outer portion of the Apennine belt and represents the most dominant structural feature in the Laga Mountains. The fault borders the Amatrice and Campotosto basins (Figs. 1 and 4).

The master fault plane is exposed in the central part of the structure, where it cuts the oldest formations exposed in the footwall. The fault zone is characterized by several slickensides dipping at a high angle (70–80°) toward the SW; its geomorphological expression (fault scarp) clearly marks its extant position (Blumetti and Guerrieri, 2007; this study). The fault is 28 km long and is conventionally divided into two segments, i.e., the Amatrice and the Campotosto faults. The two segments have lengths of 10 and 18 km, respectively (Cacciuni et al., 1995; Galadini and Messina, 2001; Galadini and Galli, 2003; Falcucci et al., 2018). According to Boncio et al. (2004a), the maximum cumulative displacement in the middle part of the fault is 2300 m, rapidly decreasing to zero at the lateral fault tips. The fault puts into contact the uppermost Burdigalian to lowermost Messinian Marne con Cerrogna formation, in the footwall, with the Messinian siliciclastic Laga Formation in the hanging wall. Boncio et al. (2004b) considered the displacement as entirely post-thrusting (i.e., Quaternary), obtaining a mean slip rate of up to 1.0 mm/yr. On the other hand, Galadini and Galli (2003) estimated a maximum slip rate of 0.7–0.9 mm/yr and considered the activation of this segment of the MGF probably later than the early Pleistocene.

TABLE 1. SUMMARY OF THE PARAMETERS USED TO MODEL THE SEISMOGENIC FAULT PLANES OF THE SEVEN STUDIED MAIN EVENTS THAT OCCURRED IN THE CAMPOTOSTO SEISMIC ZONE, CENTRAL ITALY

Date	Time (UTC)	Nodal planes			Mw	Mo (dyne cm)	L (m)	A (m²)	D (cm)
		strike	dip	rake					
4/6/2009	23:15:37	154	57	−80	5.0	3.69E + 23	2300	5.29E + 06	30
		316	34	−106					
4/9/2009	0:52:59	322	46	−95	5.2	3.46E + 23	3200	1.02E + 07	40
		149	45	−85					
4/9/2009	19:38:16	137	48	−86	5.0	8.25E + 23	2300	5.29E + 06	30
		311	42	−95					
1/18/2017	9:25:40	331	58	−91	5.1	6.39E + 23	2800	7.84E + 06	50
		153	32	−88					
1/18/2017	10:14:09	161	51	−86	5.5	2.15E + 24	4500	2.03E + 07	70
		335	39	−95					
1/18/2017	10:25:23	319	55	−91	5.4	1.42E + 24	4000	1.60E + 07	60
		140	35	−89					
1/18/2017	13:33:36	313	71	−115	5	4.14E + 23	2500	6.25E + 06	35
		188	30	−39					

Notes: (Time Domain Moment Tensor Catalogue: http://cnt.rm.ingv.it/en/tdmt; Scognamiglio et al., 2006). The geometrical parameters refer to: fault length (L), fault area (A), and maximum coseismic displacement (D, estimated for a 10 Mpa stress drop). Mw—moment magnitude; Mo—seismic moment.
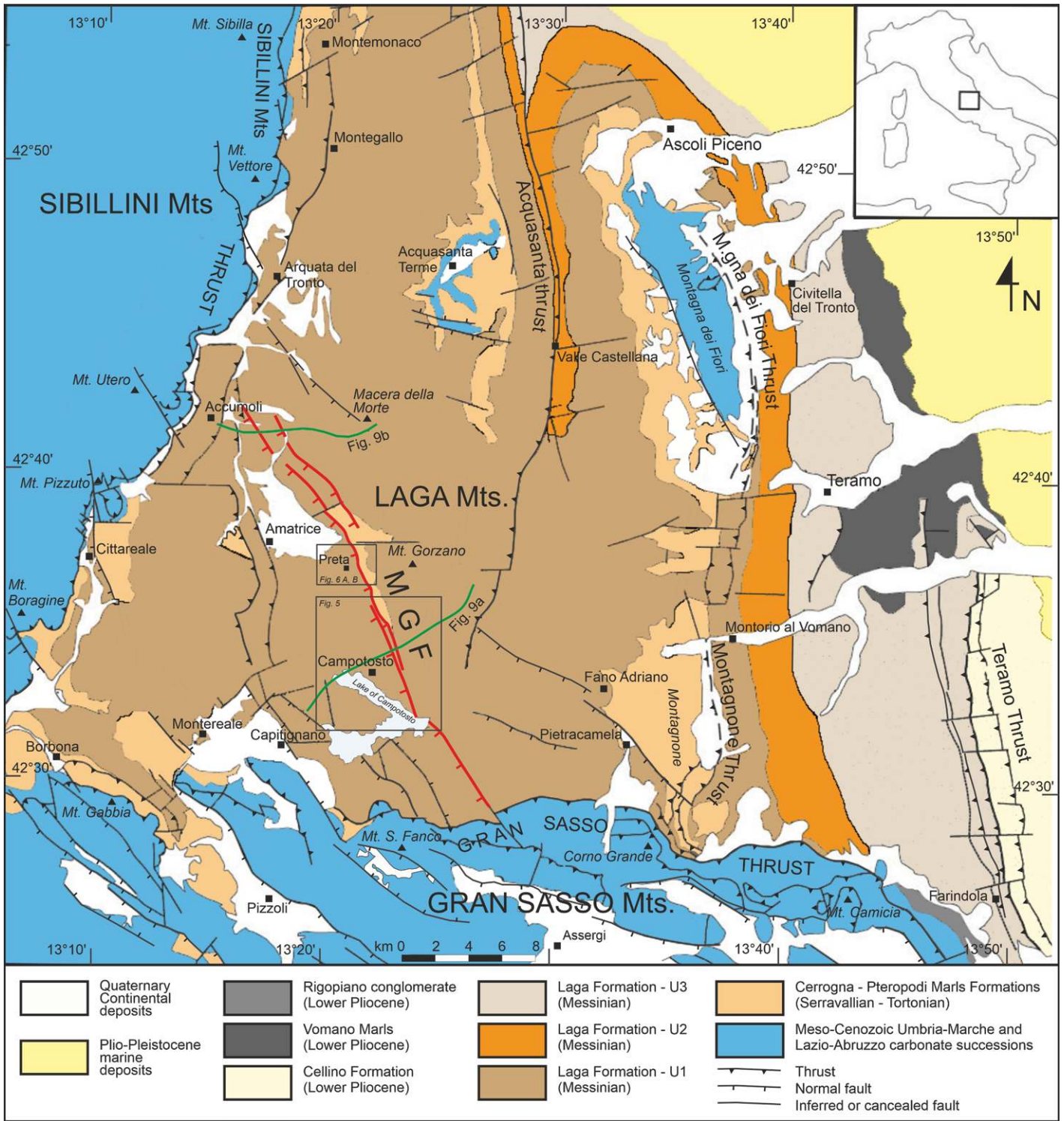
Figure 4. Geological sketch map of the Laga Basin, central Italy (Centamore et al., 1992, modified). The Monte Gorzano Fault (MGF) is in red, the Amatrice and Campotosto basins are in correspondence of the homonymous villages. The area represented in Figure 5 and the traces of the seismic profiles of Figure 8 are also shown.

The Laga Basin sits on the faulted Jurassic–upper Miocene dominantly carbonate succession. The basin has a triangular shape and is located in the footwall of the major thrusts of the region, i.e., the Umbria–Marche–Sabina thrust zone (Mazzoli et al., 2005; see also Carminati and Doglioni, 2012), or Monti Sibillini thrust to the east, and the Gran Sasso thrust to the south (Calamita et al., 2018). These thrusts were active during the deposition of the Laga Formation, which shows lateral facies variations marked by the transition from channelized

deposits in the north-western portion of the basin to lobe deposits in its eastern and south-eastern part (Milli et al., 2009; Marini et al., 2011).

In the studied area (Fig. 5), the MGF consists of a main fault plane striking NW-SE and several minor fault splays offsetting at the surface the Laga and Marne con Cerrogna formations (Figs. 5A, 6A, and 6B). The splays occur in the northernmost part of the studied area (Fig. 5). Here, the arenaceous-pelitic association of the Laga Formation, in the hanging wall, is in contact with the Marne con Cerrogna formation in the footwall, with an estimated dip separation of 900–1050 m (based on the dip angles of the projected anticline flanks; Fig. 5B, section B–B′). Moving along strike to the south-southeastern part, the stratigraphically uppermost part of the Laga Formation (i.e., the Pelitic member) occurs in the hanging wall, while the arenaceous association is exposed in the footwall (Fig. 5B, section A–A′; Fig. 6C and 6D). This yields an estimated offset of 750–780 m.

Along the southern portion of the fault, the pelitic association of the Laga Formation—consisting of thin to medium shale beds and fine- to medium-grained sandstones—often dips in opposing directions, defining folds with steep to vertical limbs in the vicinity of the main fault plane (Fig. 5A). Such folds do not occur farther NNW, where an array of splays offset the dominantly sandstone beds of the arenaceous-pelitic association located in the footwall block with respect to the principal fault plane (Fig. 5B).

The Campotosto 1 well (ViDEPI data; https://www.videpi.com/videpi/pozzi/dettaglio.asp?cod=1109), situated ~3.8 km W of the surface expression of the fault plane (Fig. 5A), penetrated a thin portion of the arenaceous association occurring on top of the arenaceous-pelitic association. The interpretation of the Campotosto 1 well data and the correlation with the outcomes of field mapping allowed us to estimate the position of several marker beds, such as a main turbiditic bed and peculiar arenaceous-pelitic levels within the arenaceous association (Fig. 5). The stratigraphic thickness between two reference datum levels (top of Orbulina Formation and the previously mentioned turbiditic marker bed) was obtained for both footwall and hanging-wall blocks. Based on field mapping, this thickness is of 750–780 m in the footwall, while the same stratigraphic portion in the hanging wall (obtained from the integration of the Campotosto 1 well and field mapping data, Fig. 5C) is in the range of 900–1050 m. This portion is therefore 150–300 m thicker in the hanging wall than in the footwall of the MGF.

DISCUSSION

The seismic sequences that occurred in the last decades in central Italy (Rovida et al., 2019; Chiaraluce et al., 2017) allowed us to (a) verify the geological and paleoseismological analyses carried out prior to the seismic events, (b) improve our knowledge of the seismotectonic setting of central Italy, and (c) better understand the interaction processes between active faults (on the long-term) and earthquakes (on the short-term) within an active fault system (i.e., the CAFS; Cello et al., 1997).

The geological surveys carried out immediately after the mainshocks of the 1997-Colfiorito-Sellano Mw = 6.0; 2009-L′Aquila Mw = 6.3, and 2016-Amatrice-Visso-Norcia Mw max = 6.5 seismic sequences documented how surface faulting and secondary coseismic phenomena are widespread (Tondi et al., 2009; Pantosti and Boncio, 2012; Civico et al., 2018; Villani et al., 2018). After the 2016-Amatrice-Visso-Norcia mainshocks, surface faulting was observed along several faults that had been previously mapped as active and capable, belonging to the Monte Vettore-Monte Bove fault system (Calamita and Pizzi, 1994; Cello et al., 1997; Pizzi et al., 2002; Pierantoni et al., 2013; Galli et al., 2016; Civico et al., 2018; Villani et al., 2018). This confirms that active and capable faults individuated at the surface can be interpreted as the manifestation of the deep seismogenic structure, from which the maximum expected magnitude can be estimated. This is based on fault dimension (previously evaluated Mw max = 6.5–6.7, see Barchi et al., 2000), according to the "areal segmentation model" of Tondi (2000). On the other hand, a different scenario is suggested for the 2009-L′Aquila earthquake (Chiarabba et al., 2009; Boncio et al., 2010; Galli et al., 2010, Pantosti and Boncio, 2012; Moro et al., 2013). Here, besides primary surface faulting along the PF (for a total rupture length of 3–12 km; e.g., Pantosti and Boncio, 2012), coseismic phenomena (e.g., free faces, open fractures) observed discontinuously along very small sections (up to few hundred meters long) of previously mapped active and capable faults (e.g., the Pettino, the Gran Sasso, and the Bazzano faults) are not directly associated with the causative seismogenic fault (i.e., the PF) of the 2009-L′Aquila mainshock (EMERGEO Working Group, 2009; EMERGEO Working Group, 2010). Rather, in this case they represent secondary phenomena due to ground shaking, facilitated by the different mechanical properties (carbonate bedrock versus loose continental deposits) of the rocks exposed in each of the fault blocks.

It is important to point out that these secondary coseismic phenomena may produce effects that are similar to those of primary surface faulting in the rejuvenation of a fault scarp, also involving the deformation of Holocene sediments and/ or the soil in some instances. As these represent some of the most important evidence commonly considered for the identification of active and capable faults, caution should be applied in the lack of a robust geological analysis (i.e., geological mapping and related structural interpretation, paleoseismological analysis). Within this framework, some of the active and capable faults mapped in the Apennines, individuated based exclusively on the evidence described above, may actually represent pre-existing structures not directly connected with the seismogenic sources. Therefore, they cannot be used in terms of seismic hazard evaluation purposes.

The recent 2016 central Italy seismic sequence provided important insights into the understanding of the seismic cycle and recurrence time of large earthquakes for the interacting and fragmented active fault systems in the Apennines (Tondi and Cello, 2003). It is well known that the seismic cycle of single faults is not regular, as fault interaction processes may anticipate or retard slip, thus affecting both time and magnitude (Mildon et al., 2017). However, a different perspective emerges by considering a faulted crustal volume (Fig. 7). Prior to the 2009-L′Aquila and the 2016-Amatrice-Visso-Norcia seismic sequences, the most significant earthquakes in central Italy—clustering in two main periods over the last millennium—were associated with the CAFS structures by Tondi and Cello (2003). The reconstructed cumulative displacement was interpreted by the latter authors as "slip and time predictable," with a recurrence time period of ~350 years for large earthquakes (M ≥ 6.5) generated by the CAFS structures. As it may be observed in Figure 7, the seismic sequences that occurred in the last decade in central Italy are in agreement with the prediction. These results may have important implications for seismic hazard analysis, in particular for the opportunity to include the "time" parameter on its evaluation.

As shown in Figure 1, the seismogenic faults responsible for the 2009-L′Aquila Mw = 6.3 (Paganica Fault—PF) and 2016-Amatrice-Visso-Norcia Mw max = 6.5 (Monte Vettore Fault—MVF) are right-stepping with a negative overlap (i.e., underlap; see also Fig. 2). This latter coincides at the surface with the area of Campotosto (Campotosto Seismic Zone—CSZ in this paper). During the 2009 seismic sequence and in 2017, few months later than the mainshocks related to the 2016 seismic sequence, the CSZ was affected by seismic swarms with
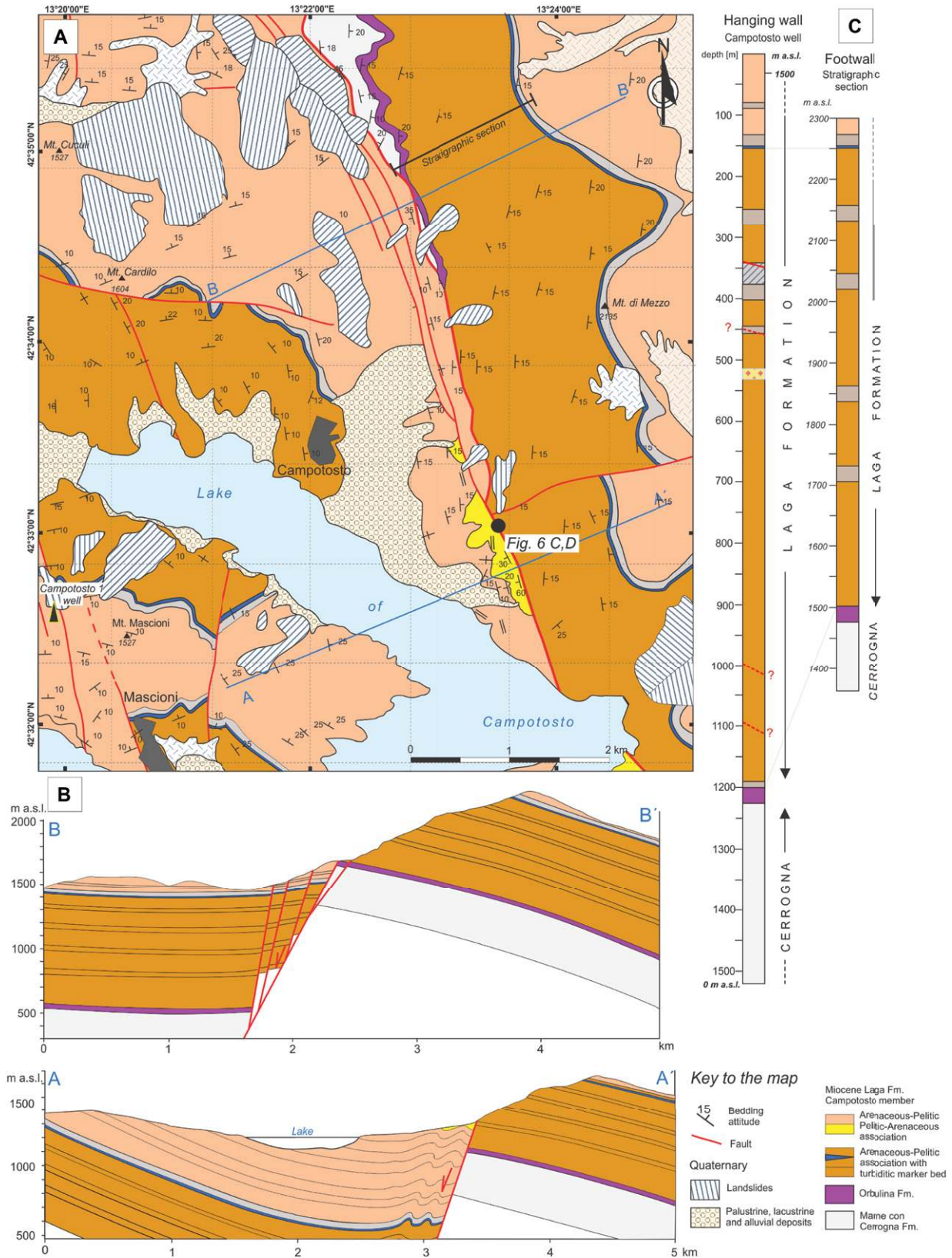
Figure 5. (A) Geological map of the Campotosto area, central Italy, with (B) cross-sections A–A′ and B–B′ (located in Fig. 6A) in the southern segment of the Monte Gorzano Fault (MGF) and (C) simplified stratigraphic columns of the hanging-wall (based on the interpretation of the well log) and footwall (based on field mapping) blocks. The location of the photos of Figure 6 (C, D) is also shown. Fm.—Formation; m a.s.l.—meters above sea level.
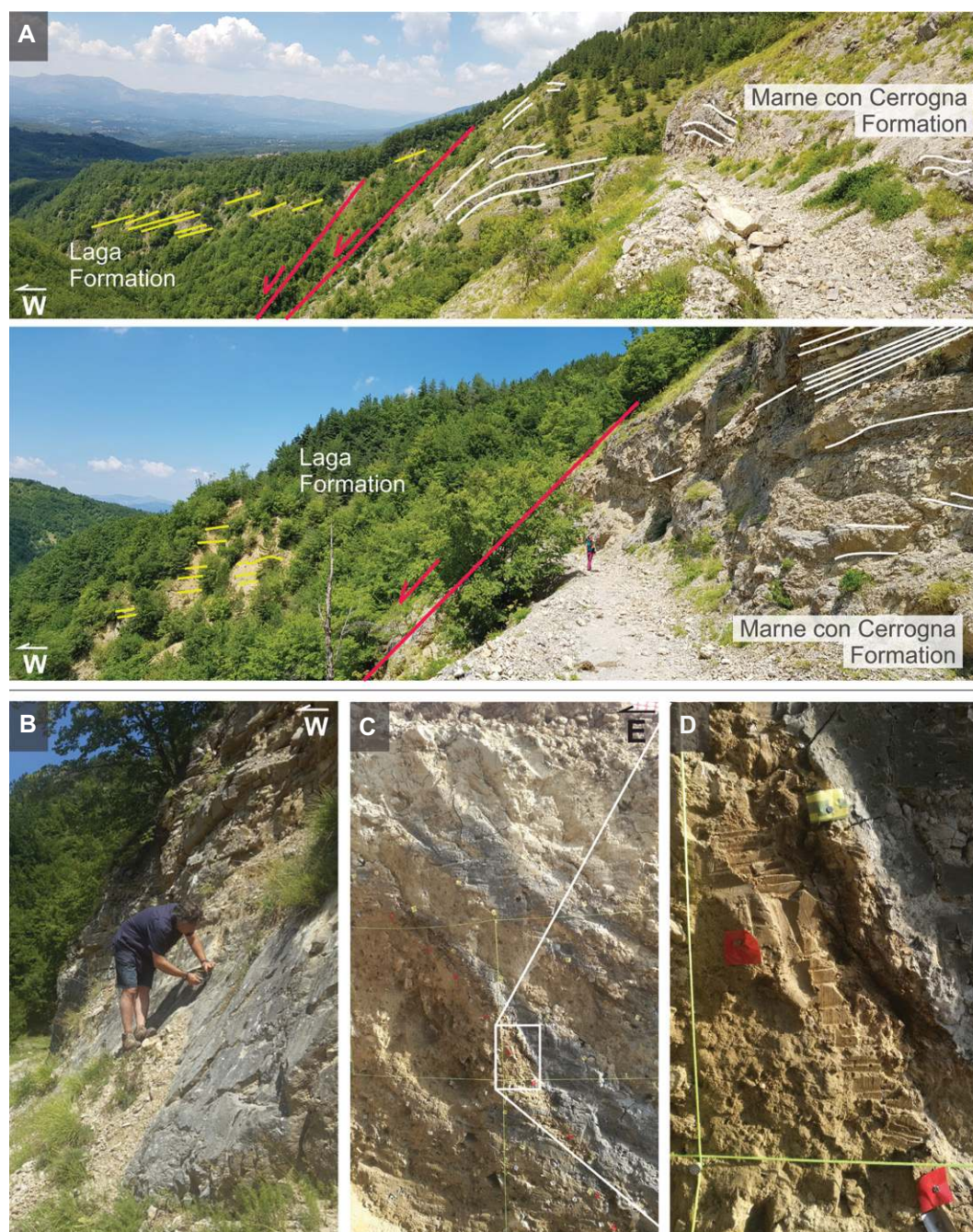
Figure 6. (A) Two general views of the Monte Gorzano Fault (MGF) exposed in the central part of the structure immediately to the east of the village of Petra, central Italy (see Fig. 4). The main fault surfaces are indicated in red and the traces of bedding of the hanging-wall and footwall blocks are also shown (note fault-related drag of bedding). The fault zone in the Marne con Cerrogna Formation is represented by a cataclastic fault core, including several slickensides, and a >10-m-thick damage zone. (B) Detail of slickensides dipping at a high angle (70–80°) toward the SW (Marne con Cerrogna Formation). (C) Fault zone associated with the fault scarp in the southern portion of the MGF (see Fig. 5 for location). The outcrop is a vertical wall of a trench excavated across the fault scarp; the fault plane puts into contact the arenaceous-pelitic association (footwall) against the pelitic association (hanging wall) of the Laga Formation. (D) Detail of the fault zone, in which a closely spaced foliation (S tectonites sensu Lister and Snoke, 1984) occurs.

magnitudes ranging from 5.0 to 5.5, thus suggesting a strong interaction between the PF and the MVF.

The seismogenic structures related to the main seismic events that occurred in the CSZ were modeled and interpreted as a linkage fault zone between the PF and MVF interacting seismogenic faults (Fig. 8). Hypocenter location within the CSZ suggests the occurrence of two different structures within the linkage zone: a northern fault, located at 5–7 km depth, is aligned with and striking in the direction of the MVF. A southern fault is right stepping with respect to the PF and located deeper (between 7 and 12 km; see also Bigi et al., 2013) with respect the northern one (Fig. 8). Based on the dimension of the underlap region between the PF and the MVF, the seismogenic potential of the CSZ is in the order of Mw = 6.0, even in the case where both structures composing the linkage zone activated simultaneously.

This feature has important implications for seismic hazard assessment in central Italy, as the CSZ has been recently considered able to generate an earthquake of maximum magnitude Mw = 6.5–7.0 (Falcucci et al., 2018).

The high-resolution seismological data related with the recent earthquake sequences of central Italy provide a 4-D picture of the crustal volume in the underlap region between two major active faults. This enhanced picture of a developing fault linkage zone points out how the tips of the major faults are surrounded by a "process zone" at the scale of the whole seismogenic crust. This "mega-process zone" includes minor—though seismogenic—fault segments that may be envisaged to play a fundamental role in the fault linkage process. This does not occur merely by the lateral propagation of the tips of the initially

N	Year	Latitude	Longitude	Epicentral zone	Imax	Me (Mw)
1	1279	43.27	12.78	Colfiorito	9	6.4
2	1328	42.85	13.02	Norcia	10	6.2
3	1349	42.17	13.38	L'Aquila	10	7
4	1599	42.72	13.00	Cascia	8.5	5.9
5	1639	42.65	13.25	Amatrice	10	6
6	1703	42.68	13.12	Norcia	11	6.7
7	1703	42.62	13.10	Montereale	8	6
8	1703	42.47	13.20	L'Aquila	10	6.6
9	1730	42.45	13.08	Leonessa	9	6.3
10	1786	42.32	13.37	L'Aquila	8	5.6
11	1859	42.79	13.01	Norcia	8.5	5.9
12	1979	42.72	13.07	Norcia	8.5	(5.8)
13	1997	43.00	12.60	Colfiorito	8	(6)
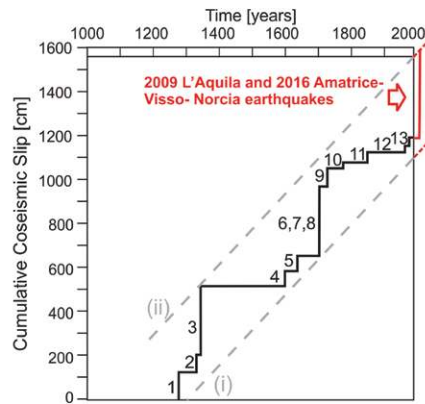
Figure 7. Graphical representation of the equivalent magnitude of the central Apennines fault system-related historical earthquakes of central Italy versus time and seismic cycle (modified after Tondi and Cello, 2003). The cumulative displacements for the 2009 L'Aquila and 2016 Amatrice-Visso-Norcia earthquakes are from Cheloni et al. (2014) and Walters et al. (2018). The historical earthquakes reported in the table are those originally included in Tondi and Cello (2003) based on seismic catalogues cited therein. Imax—maximum intensity; Me—equivalent magnitude; Mw—moment magnitude.

isolated major faults within the crustal volume comprised between them (underlap region). Rather, minor fault segments developed in the early stages of fault interaction in the underlap region are likely to grow and link up progressively, to eventually form a continuous, longer fault by joining the two preexisting major faults.

Structural Characteristics and Timing of Activity of the Monte Gorzano Fault

The MGF has been considered an active and capable fault that can generate a significant maximum magnitude (Bachetti et al., 1990; Blumetti and Guerrieri, 2007). The related influence on seismic hazard was evaluated based on fault dimensional parameters (i.e., length and cumulative displacement; Barchi et al., 2000; Boncio et al., 2004b; Falcucci et al., 2018), coupled with paleoseismological information from a single trench provided by Galadini and Galli (2003). Moreover, according to some authors (Falcucci et al., 2018), along the line of the main seismic sequences (from north to south: 1997—Umbria-Marche, 2016—Amatrice-Visso-Norcia, and 2009—L'Aquila), the Campotosto fault segment of the MGF represents a seismic gap with an associated maximum expected magnitude of the order of Mw = 6.6–6.7.

Despite this dominant interpretation, various authors proposed a different interpretation for the MGF. Tondi and Cello (2003) indicated only the northern part of the MGF as active and capable. This interpretation was based on the recent geological evolution of the Amatrice basin, that we now know is related to the seismogenic source of the Mw = 6.0 earthquake that occurred on 24

August 2016. This latter was related, by several authors, to the southern tip of the MVF seismogenic source (Anzidei and Pondrelli, 2016). Bigi et al. (2013) pointed out that the 2009 seismic swarm in the CSZ indicates the occurrence of a deep extensional structure that does not have any surface expression nor connection with the MGF. Based on the interpretation of available seismic data across the area (Fig. 9), the latter authors provided geological sections on which the MGF is shown as a shallow structure playing no role in seismogenesis. Moreover, a recent work based on tomographic data (Buttinelli et al., 2018) supports Bigi et al.'s (2013) model, confining the seismicity of the CSZ to depths in excess of 5–6 km.

Comparing the geometry and the characteristics of the MGF with other fault systems representing the surface expression of seismogenic sources of the CAFS (Tondi, 2000; Tondi and Cello, 2003), a markedly different pattern emerges. The MGF consists of a continuous—not segmented—structure showing a total length of 28 km, with well-defined and geologically homogeneous footwall and hanging blocks and a coherent displacement that can be followed with regularity from tip to tip (Boncio et al., 2004b). According to well-defined length (L) versus maximum displacement (D) scaling relationships for normal faults, classically implying D/L values in the order of 10^{-2} (Kim and Sanderson, 2005), the maximum displacement of the MGF should be less than 300 m. However, the cumulative offset in the central part of the fault would be eight times larger than that according to Boncio et al. (2004b), and is still almost six times larger according to the detailed reappraisal—based on additional field and well constraints—carried out in this study (Fig. 10).

Further active and capable fault systems exposed in the central Apennines (i.e., the Colfiorito, Norcia, and Monte Vettore-Monte Bove) include fault segments characterized by anomalously high D/L values. These occur in correspondence with pre-existing faults (of Jurassic or Miocene age) that were reactivated during Quaternary extension. In contrast to the MGF, these are short and discontinuous segments whose displacement anomalies have been clearly recognized and associated to specific pre-existing, inherited structures (Calamita and Pizzi, 1992, 1994, Pierantoni et al., 2013, Di Domenica et al., 2012). Once the displacement components associated with the pre-Quaternary activity of these fault segments is subtracted, the cumulative recent displacement of the fault systems display "conventional" D/L values in the order of 10^{-2} (Cello et al., 1998b, Kim and Sanderson, 2005).

A further issue with the large displacement associated with the MGF is represented by fault slip rate. If the displacement is considered to have occurred entirely post-thrusting, a mean slip rate of up to 1.0 mm/yr is obtained in case extension started in the early Pleistocene (Boncio et al., 2004b). On the other hand, in the case of the MGF activity occurring within the last 800 k.y., i.e., the time of widespread post-orogenic extension in the Apennines according to several authors (e.g., Cello et al., 1997; Bigi et al., 2013), the fault slip rate would exceed 3 mm/yr. Such a slip rate is one order of magnitude larger than typical slip rates calculated for active normal faults in the Apennines (e.g., Cello et al., 1997; Pizzi et al., 2002; Galli et al., 2008, Ascione et al., 2013, and references therein). This inconsistency of the MGF slip rate may be explained by considering a different tectonic scenario. The thickness variation of the Laga Formation in the hanging wall and footwall blocks suggests a synsedimentary activity of the fault during the late Miocene. A similar difference was documented by Mazzoli et al. (2002) for the Marne con Cerrogna Formation across the Montagna dei Fiori Fault, which represents a similar structure located ∼20 km to the east (Fig. 4). Both of these faults display evidence of pre-thrusting extensional activity, in the form of: (a) thickness variations of stratigraphic units across the fault, recording syn-rift sediment accommodation on top of the downthrown hanging-wall block, and (b) intense folding of the hanging-wall sedimentary fill in proximity to the fault surface, indicating buttressing against the preexisting mechanical interface represented by the fault during subsequent orogenic shortening (Calamita et al., 1998, 2018; Mazzoli et al., 2002; Scisciani et al., 2002; Butler et al., 2006; Withjack et al., 2010; Brogi, 2016). Buttressing
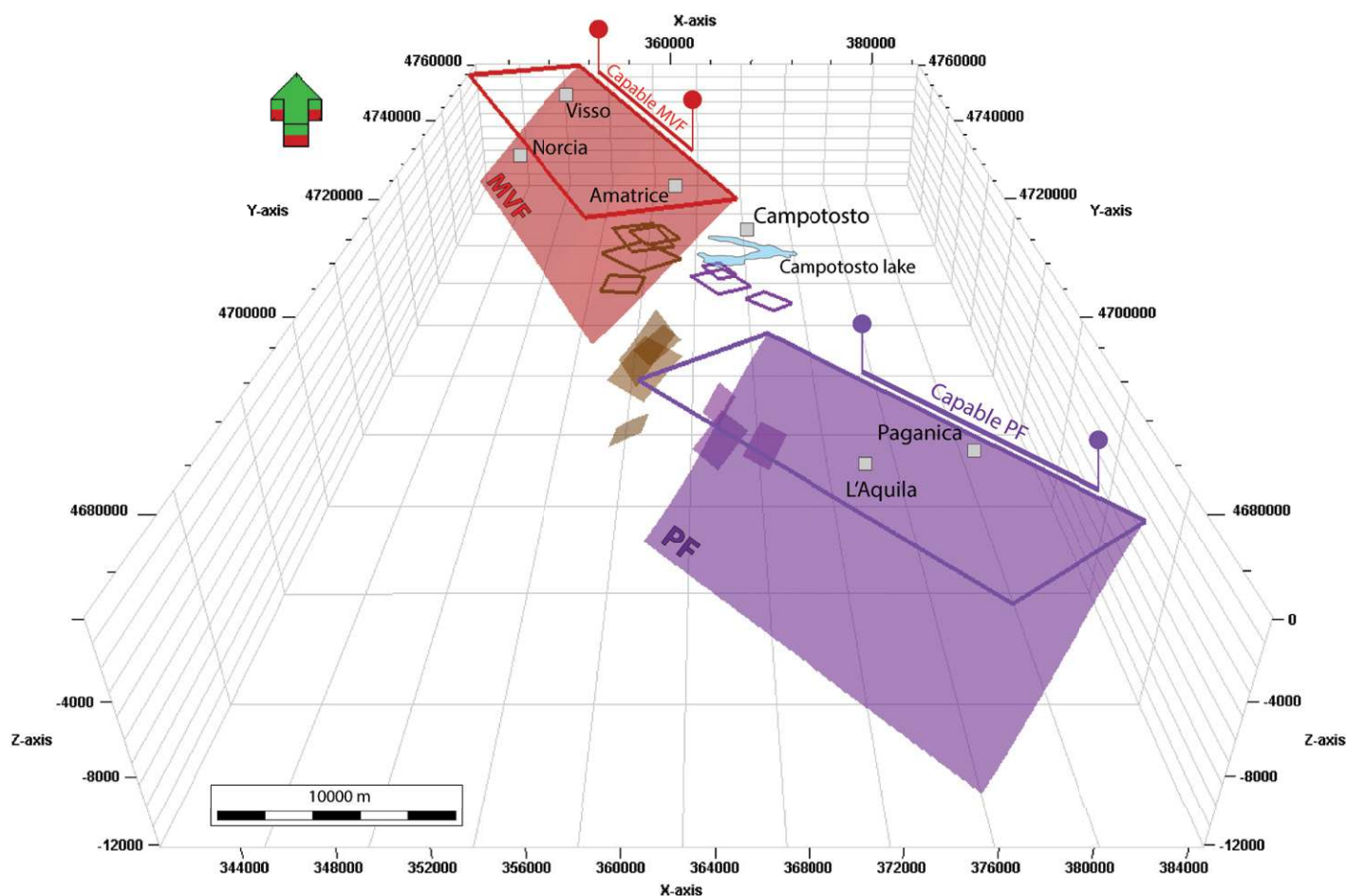
Figure 8. 3-D model of the seismogenic structures related to the 2009 L'Aquila seismic sequence (purple) and the 2016–2017 Amatrice-Visso-Norcia seismic sequence (red/brown) of central Italy. The model shows the difference in length between the capable faults at the surface and the related seismogenic sources at depth. This difference is consistent with the pronounced elliptical shape typical of normal faults (Torabi et al., 2019). The seismogenic sources of the main events (moment magnitude ≥ 5.0) that occurred in the underlap region between the two main faults outline a linkage zone beneath the Campotosto area.

may affect both hanging wall and footwall blocks, depending on the competence of the rocks (Calamita et al., 2018). In our instance, the lithologies more prone to buttressing are those of the pelitic-arenaceous association of the Laga Formation, that in fact show intense folding in the southern part of the MGF hanging wall. These features provide evidence that, during orogenic shortening, the MGF already existed, but did not undergo significant fault reactivation and positive inversion. Accordingly, we interpret the MGF as a late Miocene, pre-thrusting normal fault caused by flexure-related extension of the foreland lithosphere (Mazzoli et al., 2002; Scisciani et al., 2002). Although this evidence testifies a Miocene activity of the fault, we cannot rule out that an important amount of the cumulative vertical separation was produced at a later stage (i.e., during Pliocene–Quaternary times). Pre-thrusting normal faults of this type, interacting with the evolving thrust belt

may be either dissected by later thrusts or reactivated—entirely or partially, i.e., in segments only—during positive tectonic inversion, as diffusely documented in the Apennines (e.g., Gran Sasso Fault, Majella Fault, Montagna dei Fiori Fault, Camerino Syncline Fault and Monte San Vicino Anticline faults) (Mazzoli et al., 2002; Scisciani et al., 2002; Butler et al., 2006; Satolli et al., 2014). As with the Montagna dei Fiori Fault, the MGF is characterized by anomalous displacement-length relationships, with a dramatic tapering of extensional throw toward the fault tips (Ghisetti and Vezzani, 2000). These features were interpreted by Storti et al. (2018) as a result of further, syn-thrusting extensional fault activity triggered by gravitational re-equilibration involving the collapse of the backlimb of a thrust-related anticline over a growing antiformal stack in its subsurface. The development of new thrust sheets at depth would have caused uplift and hinterlandward tilting of the overlying

anticline, triggering extensional collapse of the thrust ramp and renewed normal fault motion. A similar interpretation also perfectly applies to the MGF, as clearly documented by the seismic evidence provided by Bigi et al. (2013) (Fig. 9). Normal faults of this type are commonly associated with the backlimbs (W flanks) of NW-SE– to NNW-SSE–trending, E vergent Apenninic macro-anticlines. Such structures are confined within thrust sheets, being bounded by the underlying thrust; therefore, they cannot play a significant role in seismic hazard.

The marked geomorphological evidence of the fault scarp associated with the MGF (Bachetti et al., 1990; Blumetti and Guerrieri, 2007), which has been used as the most important evidence for inferring fault activity, may actually be related to the differential resistance to erosion of the two fault blocks (refer to the geological map of Fig. 5). Indeed, the central Apennines include well-known examples of
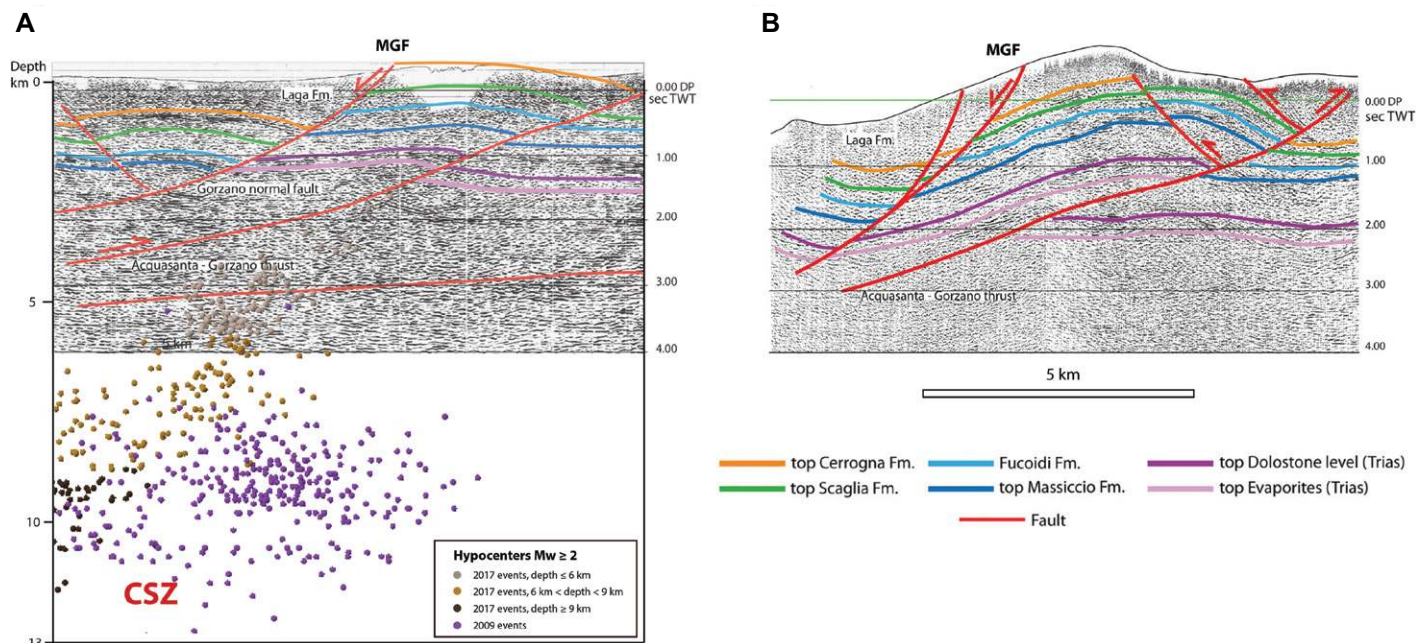
Figure 9. Interpreted seismic profiles (located in Fig. 4) after Bigi et al. (2013) showing the Monte Gorzano Fault (MGF) offsetting the backlimb of the ramp anticline associated with the Acquasanta-Gorzano thrust, central Italy. According to the latter authors, the normal fault (bifurcating into two shallow splays in B) rejoins the thrust at depth. In (A) the hypocenter distribution, projected along strike (155°) onto the seismic section, shows the Campotosto Seismic Zone (CSZ) seismicity (falling in the 5–12 km depth range) to be completely unrelated with the overlying MGF. DP—data position; Fm.—Formation; Mw—moment magnitude; TWT—two-way travel time.

large normal faults (e.g., the Montagna dei Fiori and the Leonessa faults) displaying morphologically evident fault scarps that are actually the result of lithologically controlled differential erosion; these faults are no longer considered active (e.g., Fubelli et al., 2009).

Further debatable geomorphological considerations influenced the interpretation of the recent evolution of the MGF. For example, the more pronounced morphological evidence of the fault scarp in the Campotosto area was attributed to the greater Pleistocene activity of the southern sector of the MGF (Campotosto Fault) with respect to the northern sector (Amatrice Fault) (Boncio et al., 2004b; Falcucci et al., 2018). However, the recent seismic events suggest that the evolution of the Amatrice basin is related to the southern tip of the MVF (Anzidei and Pondrelli, 2016; Tung, and Masterlark, 2018), while the Campotosto basin is related to the seismogenic sources of the CSZ. Moreover, the MGF did not show clear evidence of surface faulting during the 2016-Amatrice-Visso-Norcia seismic sequences (Aringoli et al., 2016; Livio et al., 2016; Villani et al., 2018) that strongly affected the Amatrice basin (Cheloni et al., 2019). Paleoseismological studies documented faulting of recent (Holocene) continental deposits, unique to a trench site along the MGF (Galadini and Galli, 2003). Both the fault scarp and local surface

faulting phenomena may be considered passive and associated with shaking during strong earthquakes (due to settling caused by overall sinking of the area). As already stated above, similar passive displacements occurred during the 2009-L'Aquila seismic sequence: several normal faults in the epicentral area displayed surface evidence of ruptures cutting Holocene deposits and exposure of free faces (EMERGEO Working Group, 2009; EMERGEO Working Group, 2010; Papanikolaou et al., 2010), although the seismogenic source was represented by the PF.

In any case, Holocene tectonic activity of part of the MGF at the surface cannot be completely ruled out. In fact, taking into account the structural position, a vertical linkage between the deep normal faults of the CSZ and the southern sector of the MGF is possible (Campotosto Fault, Galadini and Galli, 2003). This eventuality is supported by recent works by Falcucci et al. (2018) and Cheloni et al. (2019). The former reported new morphotectonic observations which supports evidence of an already well known "continuous major scarp" (Bachetti et al., 1990) associated with the southern sector of the MGF (i.e., the Campotosto Fault), with some morphological differences with respect to the northern one (i.e., the Amatrice Fault). According to these authors, the different morphological expression of the fault scarp in the

two sectors is related to a different and independent slip behavior of the two fault segments in recent times. As already discussed, these differences may be associated with a different slip behavior—with related surface deformation and differential erosion—of the deep seismogenic sources located beneath the two areas (i.e., the southern tip of MVF and the CSZ). Such morphological differences could be further enhanced by a linkage between the deep seismogenic sources of the CSZ and the southern sector of the MGF in the Campotosto area. Based on InSAR and GPS data, Cheloni et al. (2019) concluded that surface deformation during the 2017 Campotosto seismic swarm is compatible with a continuous fault plane from depth to the surface. However, we believe that due to the location of the deep seismogenic sources of the CSZ—with respect to the surface position of the southern sector of MGF—it is difficult to discriminate between the different possible scenarios. According to our high-resolution seismological and geological data sets acquired in relation to the recent earthquake sequences, a linkage between the deep seismogenic sources and the outcropping southern sector of the MGF is not proved, also because the geometry and the spatial relationship of the seismogenic sources of the CSZ define a large fractured zone (Fig. 3) not identifiable with a planar structure that could
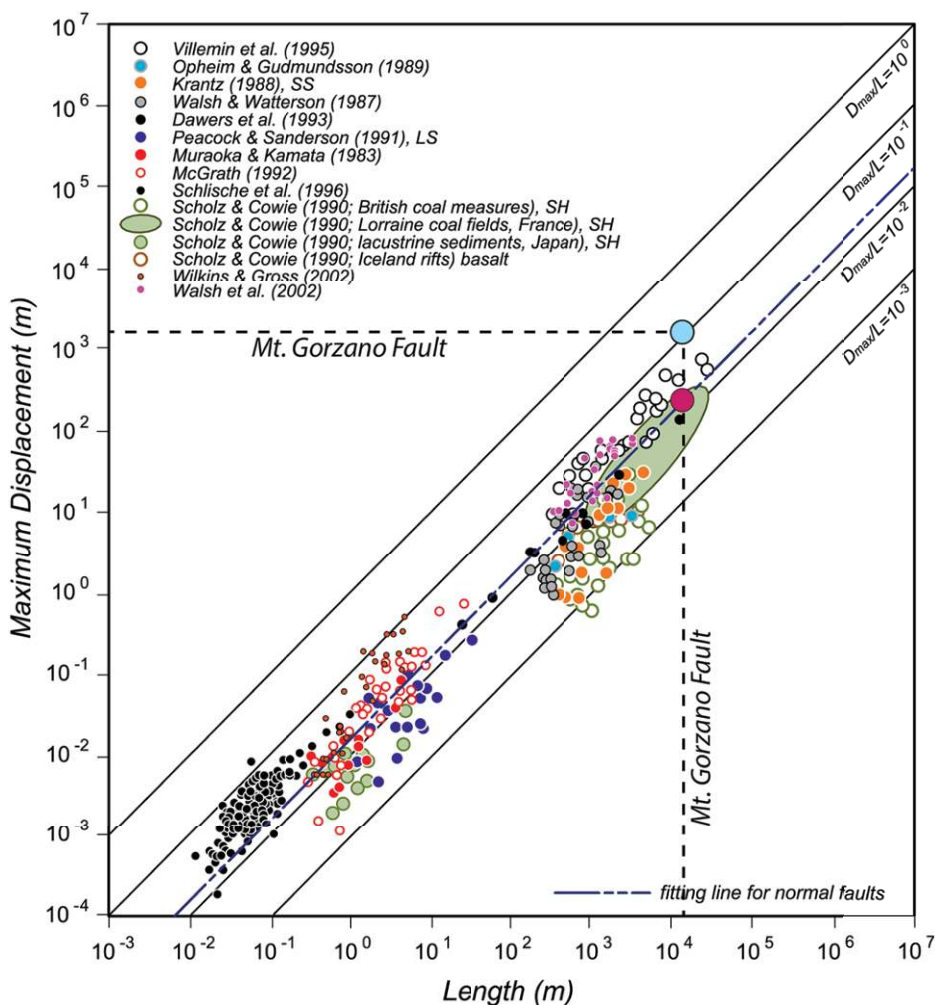
Figure 10. Plot of maximum displacement (Dmax) versus length (L) for normal and thrust faults compiled from a large number of published studies (Kim and Sanderson, 2005), showing the anomalous dimensional characteristics of the Monte Gorzano Fault, central Italy (note fitting line for normal faults). SS—sandstone; LS—limestone; SH—shale.

CONCLUSIONS

The seismic sequences that occurred in central Italy in the last decades provided new, fundamental seismological and geological constraints to: (a) verify/validate the earthquake geological studies carried out prior to the seismic events, (b) improve our knowledge on the seismotectonic setting of central Italy, and (c) better understand fault interaction and growth processes. The main outcomes of this study are listed below.

(1) The geometry, kinematics, and dimension of the seismogenic faults responsible for the largest earthquakes can be coherently evaluated by the interpretation of the highly fragmented active and capable fault system at the surface, as previously envisaged by Tondi (2000) and Boncio et al. (2004a).

(2) Coherent and interacting fault systems, composed of several seismogenic faults, can be usefully studied to obtain an estimate of the recurrence intervals for large earthquakes in regions of active extension such as the Apennines.

(3) The seismotectonic setting of the epicentral area of the 2009-L′Aquila and 2016-Amatrice-Visso-Norcia earthquakes is characterized by two interacting and growing seismogenic faults (PF and MVF), with the Campotosto linkage fault zone located in between.

(4) Based on underlap dimension, the seismogenic potential of the Campotosto area is in the order of Mw = 6.0 (even in the case where all the faults belonging to the linkage zone were activated simultaneously).

(5) The prominent structural feature exposed in the Campotosto area, i.e., the MGF, preserves evidence of early (pre- to syn-thrusting) activity and does not represent the surface expression of a seismogenic source identifiable as a seismic gap between the PF and MVF.

(6) The tips of the two major, isolated faults are surrounded by a "mega-process zone" formed by a fractured rock volume at the scale of the seismogenic crust. This volume includes seismically active minor faults that grow up progressively and may be envisaged to eventually join together to form a continuous, longer fault by linking the two preexisting major faults. The high-resolution seismological data discussed in this study suggest that the linkage of initially isolated major faults does not occur simply by the lateral propagation of their tips within the interposed crustal volume, as minor fault segments that formed in the incipient stages of fault interaction are likely to play a primary role in the composite and articulated linkage process occurring in the underlap region.

This study shows how the resolution of geological analysis for seismic hazard evaluation

easily link with the MGF at the surface. Regardless, even in the case where part of the MGF was actually reactivated during the current tectonic phase, our results demonstrate Miocene synsedimentary activity for this fault. The implications for seismic hazard assessment are that: (a) the length of the MGF cannot be used to evaluate the maximum expected magnitude of the area; (b) the possible primary surface effects cannot be scaled with the length of the MGF and are, consequently, moderate; and (c) the MGF does not represent a silent fault, nor a seismic gap.

As described above, the study region is a structurally composite area including folds and thrusts, as well as pre-, syn-, and post-thrusting normal faults. With this respect, the discontinuous, "immature" (i.e., not fully linked) fault system mapped in the study area probably results not only from the young age of post-orogenic

extension in the Apennines, but also from the decoupling effect of multiple décollement levels and strong rheological contrasts typically characterizing preexisting fold and thrust belts affected by post-orogenic extensional fault systems (e.g., Tavani, 2012; Ascione et al., 2013). We may conclude our discussion quoting Galadini and Messina (2001), who stated that not accurately defining the structural evolution of the inherited, multiply reactivated structures—such as the MGF of this study—that are common in the Apennines "would imply wrong conclusions for both the fault geometry and kinematics which may be delivered for seismotectonics and seismic hazard assessment. This typically leads to overestimating the fault length and the expected magnitude, or to the increase in the number of seismogenic sources affecting an area."

greatly benefited from the contribution of new seismological data sets provided by the earthquake sequences of the last decades. These furnished additional constraints for an effective and more circumstantial individuation of active and capable faults in central Italy, thereby leading to a more comprehensive picture of seismotectonic behavior. The crustal volume hosting an active zone of incipient linkage (underlap) between two large seismogenic faults is imaged with unprecedented resolution, in 4-D, by the recent seismological data sets. This may allow earth scientists to gain useful insights into the processes of fault interaction and related seismicity during early (Fossen and Rotevatn, 2016) linkage stages.

ACKNOWLEDGMENTS

REFERENCES CITED

Ackermann, R.V., and Schlische, R.W., 1997, Anticlustering of small normal faults around larger faults: Geology, v. 25, p. 1127–1130, https://doi.org/10.1130/0091-7613(1997)025<1127:AOSNFA>2.3.CO;2.

Amato, A., Azzara, R., Chiarabba, C., Cimini, G.B., Cocco, M., Di Bona, M., Margheriti, L., Mazza, S., Mele, F., Selvaggi, G., Basili, A., Boschi, E., Courboulex, F., Deschamps, A., Gaffet, S., Bittarelli, G., Chiaraluce, L., Piccinini, D., and Ripepe, M., 1998, The 1997 Umbria-Marche, Italy, earthquake sequence: A first look at the main shocks and aftershocks: Geophysical Research Letters, v. 25, no. 15, p. 2861–2864, https://doi.org/10.1029/98GL51842.

Anzidei, M., and Pondrelli, S., editors, 2016, The Amatrice seismic sequence: Preliminary data and results: INGV Annals of Geophysics, v. 59, Fast Track 5.

Aringoli, D., Farabollini, P., Giacopetti, M., Materazzi, M., Paggi, S., Pambianchi, G., Pierantoni, P.P., Pistolesi, E., Pitts, A., and Tondi, E., 2016, The August 24th 2016 Accumoli earthquake: Surface faulting and deep-seated gravitational slope deformation (DSGSD) in the Monte Vettore area: Annals of Geophysics, v. 59, https://doi.org/10.4401/ag-7199.

Ascione, A., Mazzoli, S., Petrosino, P., and Valente, E., 2013, A decoupled kinematic model for active normal faults: Insights from the 1980, MS = 6.9 Irpinia earthquake, southern Italy: Geological Society of America Bulletin, v. 125, p. 1239–1259, https://doi.org/10.1130/B30814.1.

Bachetti, C., Blumetti, A.M., Calderoni, G., Ridolfi, M., 1990, Attività neotettonica e palosismica nel settore meridionale dei Monti della Laga: Rendiconti Online della Società Geologica Italiana, v. 13, p. 9–16.

Barchi, M., Galadini, F., Lavecchia, G., Messina, P., Michetti, A.M., Peruzza, L., Pizzi, A., Tondi, E., and Vittori, E., 2000, Sintesi delle conoscenze sulle faglie attive in Italia Centrale: Parametrizzazione ai fini della caratterizzazione della pericolosità sismica: Rome, Italy, CNR-Gruppo Nazionale per la Difesa dai Terremoti, 62 p.

Bigi, S., Casero, P., Chiarabba, C., and Di Bucci, D., 2013, Contrasting surface active faults and deep seismogenic sources unveiled by the 2009 L'Aquila earthquake sequence (Italy): Terra Nova, v. 25, no. 1, p. 21–29, https://doi.org/10.1111/ter.12000.

Bignami, C., Valerio, E., Carminati, E., Doglioni, C., Tizzani, P., and Lanari, R., 2019, Volume unbalance on the 2016 Amatrice-Norcia (Central Italy) seismic sequence and insights on normal fault earthquake mechanism: Scientific Reports, v. 9, no. 4250, https://doi.org/10.1038/s41598-019-40958-z.

Blumetti, A.M., and Guerrieri, L., 2007, Fault-generated mountain fronts and the identification of fault segments: Implications for seismic hazard assessment: Bollettino della Società Geologica Italiana, v. 126, no. 2, p. 307–322.

Boncio, P., Lavecchia, G., and Pace, B., 2004a, Defining a model of 3D seismogenic sources for seismic hazard assessment applications: The case of central Apennines (Italy): Journal of Seismology, v. 8, p. 407–425, https://doi.org/10.1023/B:JOSE.0000038449.78801.05.

Boncio, P., Lavecchia, G., Milana, G., and Rozzi, B., 2004b, Seismogenesis in Central Apennines, Italy: An integrated analysis of minor earthquake sequences and structural data in the Amatrice-Campotosto area: INGV Annals of Geophysics, v. 47, no. 6, p. 1723–1742.

Boncio, P., Pizzi, A., Brozzetti, G., Pomposo, G., Lavecchia, G., Di Naccio, D., and Ferrarini, F., 2010, Co-seismic ground deformation of the 6 April 2009 L'Aquila earthquake (central Italy, Mw6.3): Geophysical Research Letters, v. 37, no. 6, https://doi.org/10.1029/2010GL042807.

Brogi, A., 2016, Influence of syn-sedimentary faults on orogenic structures in a collisional belt: Insights from the inner zone of the Northern Apennines (Italy): Journal of Structural Geology, v. 86, p. 75–94, https://doi.org/10.1016/j.jsg.2016.03.006.

Butler, R.W.H., Tavarnelli, E., and Grasso, M., 2006, Structural inheritance in mountain belts: An Alpine-Apennine perspective: Journal of Structural Geology, v. 28, no. 11, p. 1893–1908, https://doi.org/10.1016/j.jsg.2006.09.006.

Buttinelli, M., Pezzo, G., Valoroso, L., De Gori, P., and Chiarabba, C., 2018, Tectonics inversions, fault segmentation, and triggering mechanisms in the central Apennines normal fault system: Insights from high-resolution velocity models: Tectonics, v. 37, no. 11, p. 4135–4149, https://doi.org/10.1029/2018TC005053.

Cacciuni A., Centamore, E., Di Stefano, R., Dramis, F., 1995, Evoluzione morfotettonica della conca di Amatrice: Studi Geologici Camerti, special volume, no. 2, p. 95–100.

Calamita, F., and Pizzi, A., 1992, Tettonica Quaternaria nella dorsale appenninica Umbro-Marchigiana e bacini intrappenninici associate: Studi Geologici Camerti, no. 1, p. 17–25.

Calamita, F., and Pizzi, A., 1994, Recent and active extensional tectonics in the Southern Umbrio-Marchean Apennines (Central Italy): Memorie della Societa Geologica Italiana, v. 48, p. 541–548.

Calamita, F., Pizzi, A., Ridolfi, M., Rusciadelli, G., and Scisciani, V., 1998, Il buttressing delle faglie sinsedimentarie pre-thrusting sulla strutturazione neogenica della catena appenninica: L'esempio della M.gna dei Fiori (Appennino Centrale esterno): Bollettino della Società Geologica Italiana, v. 117, p. 725–745.

Calamita, F., Di Domenica, A., and Pace, P., 2018, Macro- and meso-scale structural criteria for identifying pre-thrusting normal faults within foreland fold-and-thrust belts: Insights from the Central-Northern Apennines (Italy): Terra Nova, v. 30, no. 1, p. 50–62, https://doi.org/10.1111/ter.12307.

Calderoni, G., Rovelli, A., and Singh, S.K., 2013, Stress drop and source scaling of the 2009 April L'Aquila earthquakes: Geophysical Journal International, v. 192, no. 1, p. 260–274, https://doi.org/10.1093/gji/ggs011.

Calderoni, G., Rovelli, A., and Di Giovambattista, R., 2017, Rupture directivity of the strongest 2016–2017 central Italy earthquakes: Journal of Geophysical Research. Solid Earth, v. 122, p. 9118–9131, https://doi.org/10.1002/2017JB014118.

Carminati, E., and Doglioni, C., 2012, Alps vs. Apennines: The paradigm of a tectonically asymmetric Earth: Earth-Science Reviews, v. 112, p. 67–96, https://doi.org/10.1016/j.earscirev.2012.02.004.

Cartwright, J.A., Trudgill, B.D., and Mansfield, C.S., 1995, Fault growth by segment linkage: An explanation for scatter in maximum displacement and trace length data from the Canyonlands grabens of SE Utah: Journal of Structural Geology, v. 17, p. 1319–1326, https://doi.org/10.1016/0191-8141(95)00033-A.

Castelli, V., Camassi, R., Caracciolo, C.H., Locati, M., Meletti, C., and Rovida, A., 2016, New insights in the seismic history of Monti della Laga area: INGV Annals of Geophysics, v. 59, Fast Track 5, 6 p., https://doi.org/10.4401/ag-7243.

Cello, G., Mazzoli, S., Tondi, E., and Turco, E., 1997, Active tectonics in the central Apennines and possible implications for seismic hazard analysis in peninsular Italy: Tectonophysics, v. 272, p. 43–68, https://doi.org/10.1016/S0040-1951(96)00275-2.

Cello, G., Mazzoli, S., and Tondi, E., 1998a, The crustal fault structure responsible for the 1703 seismic sequence of central Italy: Journal of Geodynamics, v. 26, no. 2–4, p. 443–460, https://doi.org/10.1016/S0264-3707(97)00051-3.

Cello, G., Deiana, G., Mangano, P., Mazzoli, S., Tondi, E., Ferreli, L., Maschio, L., Michetti, A.M., Serva, L., and Vittori, E., 1998b, Evidence of surface faulting during the September 26, 1997, Colfiorito (Central Italy) earthquakes: Journal of Earthquake Engineering, v. 2, no. 2, p. 303–324, https://doi.org/10.1080/13632469809350324.

Centamore, E., Adamoli, L., Berti, D., Bigi, S., Casnedi, R., Cantalamessa, G., Fumanti, F., Morelli, C., Micarelli, A., Micarelli, A., Ridolfi, M., Salvucci, R., Chiocchini, M., Mancinelli, A., and Potetti, M., 1992, Carta geologica dei bacini della Laga e del Cellino e dei rilievi carbonatici circostanti (Marche meridionali, Lazio nordorientale, Abruzzo settentrionale): Firenze, Italy, S.E.L.C.A., scala 1:100,000.

Cheloni, D., Giuliani, R., D'Anastasio, E., Atzori, S., Walters, R.J., Bonci, L., D'Agostino, N., Mattone, M., Calcaterra, S., Gambino, P., Dennino, F., Maseroli, R., and Stefanelli, R., 2014, Coseismic and post-seismic slip of the 2009 L'Aquila (central Italy) Mw 6.3 earthquake and implications for seismic potential along the Campotosto fault from joint inversion of high-precision levelling, InSAR and GPS data: Tectonophysics, v. 622, p. 168–185, https://doi.org/10.1016/j.tecto.2014.03.009.

Cheloni, D., D'Agostino, N., Scognamiglio, L., Tinti, E., Bignami, C., Avallone, A., Giuliani, R., Calcaterra, S., Gambino, P., and Mattone, M., 2019, Heterogeneous behavior of the Campotosto normal fault (central Italy) imaged by InSAR GPS and strong-motion data: insights from the 18 January 2017 events: Remote Sensing, v. 11, no. 1482, https://doi.org/10.3390/rs11121482.

Chiarabba, C., Amato, A., Anselmi, M., Baccheschi, P., Bianchi, I., Cattaneo, M., Cecere, G., Chiaraluce, L., Ciaccio, M.G., De Gori, P., De Luca, G., Di Bona, M., Di Stefano, R., Faenza, L., Govoni, A., Improta, L., Lucente, F.P., Marchetti, A., Margheriti, L., Mele, F., Michelini, A., Monachesi, G., Moretti, M., Pastori, M., Piana Agostinetti, N., Piccinini, D., Roselli, P., Seccia, D., and Valoroso, L., 2009, The 2009 L'Aquila (central Italy) Mw6.3 earthquake: Main shock and aftershocks: Geophysical Research Letters, v. 36, no. 18, https://doi.org/10.1029/2009GL039627.

Chiarabba, C., De Gori, P., Cattaneo, M., Spallarossa, D., and Segou, M., 2018, Faults geometry and the role of fluids in the 2016-2017 Central Italy seismic sequence: Geophysical Research Letters, v. 45, no. 14, p. 6963–6971, https://doi.org/10.1029/2018GL077485.

Chiaraluce, L., Valoroso, L., Piccinini, D., Di Stefano, R., and De Gori, P., 2011, The anatomy of the 2009 L'Aquila normal fault system (central Italy) imaged by high resolution foreshock and aftershock locations: Journal of Geophysical Research. Solid Earth, v. 116, no. B12, https://doi.org/10.1029/2011JB008352.

Chiaraluce, L., Di Stefano, R., Tinti, E., Scognamiglio, L., Michele, M., Casarotti, E., Cattaneo, M., De Gori, P., Chiarabba, C., Monachesi, G., Lombardi, A., Valoroso, L., Latorre, D., and Marzorati, S., 2017, The 2016 Central Italy seismic sequence: A first look at the mainshocks, aftershocks and source models: Seismological Research Letters, v. 88, no. 3, https://doi.org/10.1785/0220160221.

Civico, R., Pucci, S., Villani, F., Pizzimenti, L., De Martini, P.M., and Nappi, R., and the Open EMERGEO Working Group 2018, Surface ruptures following the 30 October 2016 Mw 6.5 Norcia earthquake, central Italy: Journal of Maps, vol. 14, p. 151–160, https://doi.org/10.1080/17445647.2018.1441756.

Cowie, P.A., and Roberts, G.P., 2001, Constraining slip rates and spacings for active normal faults: Journal of

Structural Geology, v. 23, p. 1901–1915, https://doi .org/10.1016/S0191-8141(01)00036-0.

Dawers, N.H., Anders, M.H., and Scholz, C.H., 1993, Growth of normal faults: displacement–length scaling: Geology, v. 21, no. 12, p. 1107–1110, https://doi .org/10.1130/0091-7613(1993)021<1107:GONFDL >2.3.CO;2.

Di Domenica, A., Turtù, A., Satolli, S., and Calamita, F., 2012, Relationships between thrusts and normal faults in curved belts: New insight in the inversion tectonics of the Central-Northern Apennines (Italy): Journal of Structural Geology, v. 42, p. 104–117, https://doi .org/10.1016/j.jsg.2012.06.008.

Doglioni, C., Carminati, E., Petricca, P., and Riguzzi, F., 2015, Normal fault earthquakes or graviquakes: Scientific Reports, v. 5, no. 12110, https://doi.org/10.1038/ srep12110.

EMERGEO Working Group, 2009, Rilievi geologici nell'area epicentrale della sequenza sismica dell'Aquilano del 6 Aprile 2009: Quaderni di Geofisica, v. 70.

EMERGEO Working Group, 2010, Evidence for surface rupture associated with the M$_W$ 6.3 L'Aquila earthquake sequence of April 2009 (central Italy): Terra Nova, v. 22, p. 43–51, https://doi.org/10.1111/j.1365-3121.2009.00915.x.

Falcucci, E., Gori, S., Bignami, C., Pietrantonio, G., Melini, D., Moro, M., Saroli, M., and Galadini, F., 2018, The Campotosto Seismic gap in between the 2009 and 2016–2017 seismic sequences of central Italy and the role of inherited lithospheric faults in regional seismotectonic settings: Tectonics, v. 37, no. 8, p. 2425–2445, https://doi.org/10.1029/2017TC004844.

Fossen, H., and Rotevatn, A., 2016, Fault linkage and relay structures in extensional settings: A review: Earth-Science Reviews, v. 154, p. 14–28, https://doi .org/10.1016/j.earscirev.2015.11.014.

Fubelli, G., Gori, S., Falcucci, E., Galadini, F., and Messina, P., 2009, Geomorphic signatures of recent normal fault activity versus geological evidence of inactivity: Case studies from the central Apennines (Italy): Tectonophysics, v. 476, no. 1–2, p. 252–268, https://doi .org/10.1016/j.tecto.2008.10.026.

Galadini, F., 1999, Pleistocene changes in the central Apennine fault kinematics: A key to decipher active tectonics in central Italy: Tectonics, v. 18, no. 5, p. 877–894, https://doi.org/10.1029/1999TC900020.

Galadini, F., and Galli, P., 2000, Active tectonics in the central Apennines (Italy): Input data for seismic hazard assessment: Natural Hazards, v. 22, no. 3, p. 225–268, https://doi.org/10.1023/A:1008149531980.

Galadini, F., and Messina, P., 2001, Plio-Quaternary changes of the normal fault architecture in the central Apennines (Italy): Geodinamica Acta, v. 14, no. 6, p. 321–344, https://doi.org/10.1080/09853111.2001.10510727.

Galadini, F., and Galli, P., 2003, Paleoseismology of silent faults in the Central Apennines (Italy): The Mt. Vettore and Laga Mts. faults: INGV Annals of Geophysics, v. 46, no. 5, p. 815–836, https://doi.org/10.4401/ag-3457.

Galderisi, A., and Galli, P., 2020, Coulomb stress transfer between parallel faults. The case of Norcia and Mt Vettore normal faults (Italy, 2016 Mw 6.6 earthquake): Results in Geophysical Sciences, v. 1–4, no. 100003, https://doi .org/10.1016/j.ringps.2020.100003.

Galli, P., Pantosti, D., and Galadini, F., 2008, Twenty years of paleoseismology in Italy: Earth-Science Reviews, v. 88, no. 1, p. 89–117, https://doi.org/10.1016/ j.earscirev.2008.01.001.

Galli, P., Giaccio, B., and Messina, P., 2010, The 2009 central Italy earthquake seen through 0.5 Myr-long tectonic history of the L'Aquila faults system: Quaternary Science Reviews, v. 29, no. 27, p. 3768–3789, https://doi .org/10.1016/j.quascirev.2010.08.018.

Galli, P., Peronace, E., Bramerini, F., Castenetto, S., Naso, G., Cassone, F., Pallone, F., 2016, The MCS intensity distribution of the devastating 24 August 2016 earthquake in central Italy (MW 6.2): INGV Annals of Geophysics, v. 59, Fast Track 5, https://doi.org/10.4401/ag-7287.

Galli, P., Castenetto, S., and Peronace, E., 2017, The macroseismic intensity distribution of the 30 October 2016 earthquake in central Italy (Mw 6.6): Seismotectonic implications: Tectonics, v. 36, p. 2179–2191, https:// doi.org/10.1002/2017TC004583.

Galli, P., Galderisi, A., Ilardoc, I., Piscitelli, S., Sciontic, V., Bellanova, J., and Calzoni, F., 2018, Holocene paleoseismology of the Norcia fault system (Central Italy): Tectonophysics, v. 745, p. 154–169, https://doi .org/10.1016/j.tecto.2018.08.008.

Ghisetti, F., and Vezzani, L., 2000, Detachments and normal faulting in the Marche fold-and- thrust belt (central Apennines, Italy): Inferences on fluid migration paths: Journal of Geodynamics, v. 29, p. 345–369, https://doi .org/10.1016/S0264-3707(99)00057-5.

Gupta, A., and Scholz, C.H., 2000, A model of normal fault interaction based on observations and theory: Journal of Structural Geology, v. 22, p. 865–879, https://doi .org/10.1016/S0191-8141(00)00011-0.

International Atomic Energy Agency (IAEA), 2010, Seismic Hazards in Site Evaluation for Nuclear Installations: Vienna, Austria, IAEA Safety Standards Series No. SSG-9.

Kim, Y.S., and Sanderson, D.J., 2005, The relationship between displacement and length of faults: A review: Earth-Science Reviews, v. 68, no. 3–4, p. 317–334, https://doi.org/10.1016/j.earscirev.2004.06.003.

King, G.C.P., and Deves, M.H., 2015, Fault interaction, earthquake stress changes and the evolution of seismicity, *in* Schubert, G., ed., Treatise on Geophysics (Second Edition): Oxford, UK, Elsevier, v. 4, p. 243–271, https://doi.org/10.1016/B978-0-444-53802-4.00077-4.

Krantz, R.W., 1988, Multiplc fault sets and three-dimensional strain: theory and application: Journal of Structural Geology, v. 10, p. 225–237, https://doi.org/10.1016/0191-8141(88)90056-9.

Lister, G.S., and Snoke, A., 1984, S-C mylonites: Journal of Structural Geology, v. 6, p. 617–638, https://doi .org/10.1016/0191-8141(84)90001-4.

Livio, F., Michetti, A.M., Vittori, E.L., Piccardi, L., Tondi, E., and Roberts, G., Central Italy Earthquake Working Group, 2016, Surface faulting during the August 24, 2016, central Italy earthquake (Mw 6.0): Preliminary results: Annals of Geophysics, v. 59, https://doi .org/10.4401/ag-7197.

Marini, M., Milli, S., and Moscatelli, M., 2011, Facies and architecture of the Lower Messinian turbidite lobe complexes from the Laga Basin (central Apennines, Italy): Journal of Mediterranean Earth Sciences, v. 3, p. 45–72, https://doi.org/10.3304/JMES.2011.005.

Mariucci, M.T., Montone, P., and Pierdominici, S., 2010, Present-day stress in the surroundings of 2009 L'Aquila seismic sequence (Italy): Geophysical Journal International, v. 182, no. 2, p. 1096–1102, https://doi .org/10.1111/j.1365-246X.2010.04679.x.

Mariucci, M.T., and Montone, P., 2016, Contemporary stress field in the area of the 2016 Amatrice seismic sequence (central Italy): INGV Annals of Geophysics, v. 59, Fast Track 5, https://doi.org/10.4401/ag-7235.

Marrett, R.A., and Allmendinger, R.W., 1990, Kinematic analysis of fault-slip data: Journal of Structural Geology, v. 12, p. 973–986, https://doi.org/10.1016/0191-8141(90)90093-E.

Mazzoli, S., Deiana, G., Galdenzi, S., and Cello, G., 2002, Miocene fault-controlled sedimentation and thrust propagation in the previously faulted external zones of the Umbria-Marche Apennines, Italy: European Geosciences Union, Stephan Mueller Special Publication Series, v. 1, p. 195–209, https://doi.org/10.5194/ smsps-1-195-2002.

Mazzoli, S., Pierantoni, P.P., Borraccini, F., Paltrinieri, W., and Deiana, G., 2005, Geometry, segmentation pattern and displacement variations along a major Apennine thrust zone, central Italy: Journal of Structural Geology, v. 27, p. 1940–1953, https://doi.org/10.1016/ j.jsg.2005.06.002.

McGrath, A., 1992, Fault propagation and growth; a study of the Triassic and Jurassic from Watchet and Kilve, North Somerset [M.S. thesis]: London, Royal Holloway, University of London, 165 p.

Mildon, Z.K., Roberts, G.P., Faure Walker, J.P., and Iezzi, F., 2017, Coulomb stress transfer and fault interaction over millennia on non-planar active normal faults: The Mw=6.5–5.0 seismic sequence of 2016–2017, central Italy: Geophysical Journal International, v. 210, p. 1206–1218, https://doi.org/10.1093/gji/ggx213.

Milli, S., Moscatelli, M., Marini, M., and Stanzione, O., 2009, The Messinian turbidite deposits of the Laga basin (central Apennines, Italy), *in* Pascucci, V., and Andreucci, S., eds., Field Trip Guide Book: Post-conference trip FT12, 27th International Association of Sedimentologists Meeting of Sedimentology, Alghero, Italy, September 20–23, p. 279–297.

Moro, M., Saroli, M., Galadini, F., Falcucci, E., Gori, S., and Salvi, S., 2013, Historical earthquakes and variable kinematic behaviour of the 2009 L'Aquila seismic event (central Italy) causative fault, revealed by paleoseismological investigations: Tectonophysics, v. 583, p. 131–144, https://doi.org/10.1016/j.tecto.2012.10.036.

Muraoka, H., and Kamata, H., 1983, Displacement distribution along minor fault traces: Journal of Structural Geology, v. 5, p. 483–495, https://doi .org/10.1016/0191-8141(83)90054-8.

Opheim, J.A., and Gudmundsson, A., 1989, Formation and geometry of fractures, and related volcanism, of the Krafla fissure swarm, northeast Iceland: Geological Society of America Bulletin, v. 101, p. 1608–1622, https:// doi.org/10.1130/0016-7606(1989)101<1608:FAGOFA >2.3.CO;2.

Pantosti, D., and Boncio, P., 2012, Understanding the April 6th, 2009 L'Aquila earthquake-the geological contribution: Italian Journal of Geosciences, v. 131, no. 3, p. 303–308, https://doi.org/10.3301/IJG.2012.25.

Papanikolaou, D.I., Lekkas, D.E., Roberts, P.G., McGuire, B., Fountoulis, G.I., Parcharidis, I., and Foumelis, M., 2010, The 2009 L'Aquila earthquake: Findings and implications: London, UK, Aon Benfield UCL Hazard Research Centre, Event Science Report 02, 33 p.

Peacock, D.C.P., and Sanderson, D.J., 1991, Displacements, segment linkage and relay ramps in normal fault zones: Journal of Structural Geology, v. 13, no. 6, p. 721–733, https://doi.org/10.1016/0191-8141(91)90033-F.

Pierantoni, P.P., Deiana, G., and Galdenzi, S., 2013, Stratigraphic and structural features of the Sibillini Mountains (Umbria-Marche Apennines, Italy): Italian Journal of Geosciences, v. 132, no. 3, p. 497–520, https://doi .org/10.3301/IJG.2013.08.

Pino, N.A., Convertito, V., and Madariaga, R., 2019, Clock advance and magnitude limitation through fault interaction: The case of the 2016 central Italy earthquake sequence: Scientific Reports, v. 9, no. 5005, https://doi .org/10.1038/s41598-019-41453-1.

Pizzi, A., Calamita, F., Coltorti, M., and Pieruccini, P., 2002, Quaternary normal faults, intramontane basins and seismicity in the Umbria-Marche- Abruzzi Apennine Ridge (Italy): Contribution of neotectonic analysis to seismic hazard assessment [Bollettino della Societa Geologica Italiana]: Italian Journal of Geosciences, v. 1, no. 2, p. 923–929.

Pizzi, A., Di Domenica, A., Gallovič, F., Luzi, L., and Puglia, R., 2017, Fault segmentation as constraint to the occurrence of the main shocks of the 2016 central Italy seismic sequence: Tectonics, v. 36, p. 2370–2387, https:// doi.org/10.1002/2017TC004652.

Roberts, G.P., Cowie, P., Papanikolaou, I., and Michetti, A.M., 2004, Fault scaling relationships, deformation rates and seismic hazards: An example from the Lazio-Abruzzo Apennines, central Italy: Journal of Structural Geology, v. 26, no. 2, p. 377–398, https:// doi.org/10.1016/S0191-8141(03)00104-4.

Rovida, A., Locati, M., Camassi, R., Lolli, B., and Gasperini, P., 2019, Catalogo parametrico dei terremoti Italiani (CPTI15), version 2.0: Istituto Nazionale di Geofisica e Vulcanologia, https://doi.org/10.13127/ CPTI/CPTI15.2.

Satolli, S., Pace, P., Viandante, M.G., and Calamita, F., 2014, Lateral variations in tectonic style across cross-strike discontinuities: An example from the Central Apennines belt (Italy): International Journal of Earth Sciences, v. 103, no. 8, p. 2301–2313, https://doi.org/10.1007/ s00531-014-1052-3.

Schlische, R.W., Young, S.S., Ackermann, R.V., and Gupta, A., 1996, Geometry and scaling relations of a population of very small rift-related normal faults: Geology, v. 24, p. 683–686, https://doi .org/10.1130/0091-7613(1996)024<0683:GASROA >2.3.CO;2.

Scholz, C., and Cowie, P., 1990, Determination of total strain from faulting using slip measurements: Nature, v. 346, p. 837–839, https://doi .org/10.1038/346837a0.

Scisciani, V., Tavarnelli, E., Calamita, F., and Paltrinieri, W., 2002, Pre-thrusting normal faults within synorogenic basins of the Outer Central Apennines,

Italy: Implications for Apennine tectonics: Bollettino Della Società Geologica Italiana, Volume Speciale, v. 1, p. 295–304.

Scognamiglio, L., Tinti, E., Quintiliani, M. 2006, Time domain moment tensor [data set]: Istituto Nazionale di Geofisica e Vulcanologia, https://doi.org/10.13127/TDMT .

Soliva, R., and Benedicto, A., 2004, A linkage criterion for segmented normal faults: Journal of Structural Geology, v. 26, p. 2251–2267, https://doi.org/10.1016/j.jsg.2004.06.008.

Soliva, R., Benedicto, A., and Maerten, L., 2006, Spacing and linkage of confined normal faults: importance of mechanical thickness: Journal of Geophysical Research. Solid Earth, v. 111, no. B1, https://doi.org/10.1029/2004JB003507.

Spina, V., Tondi, E., Galli, P., Mazzoli, S., and Cello, G., 2008, Quaternary fault segmentation and interaction in the epicentral area of the 1561 earthquake (Mw=6.4), Vallo di Diano, southern Apennines, Italy: Tectonophysics, v. 453, p. 233–245, https://doi.org/10.1016/j.tecto.2007.06.012.

Spina, V., Tondi, E., Galli, P., and Mazzoli, S., 2009, Faults growth and interaction in a seismic gap area: Implications for the seismic hazards of the Calabrian-Lucania border (southern Italy): Tectonophysics, v. 476, p. 357–369, https://doi.org/10.1016/j.tecto.2009.02.001.

Stein, R.S., King, G.C.P., and Lin, J., 1992, Change in failure stress on the southern San Andreas fault system caused by the 1992 magnitude = 7.4 Landers earthquake: Science, v. 258, no. 5086, p. 1328–1332, https://doi.org/10.1126/science.258.5086.1328.

Stein, R.S., Barka, A.A., and Dieterich, J.H., 1997, Progressive failure on the North Anatolian fault since 1939 by earthquake stress triggering: Geophysical Journal International, v. 128, no. 3, p. 594–604, https://doi.org/10.1111/j.1365-246X.1997.tb05321.x.

Stein, S., and Wysession, M., 2003, An Introduction to Seismology, Earthquakes, and Earth Structure: Oxford, UK, Blackwell, p. 52.

Stemberk, J., Dal Moro, G.C., Stemberk, J., Blahůt, J., Coubal, M., Košťák, B., Zambrano, M., and Tondi, E., 2019, Strain monitoring of active faults in the central Apennines (Italy) during the period 2002–2017: Tectonophysics, v. 750, p. 22–35, https://doi.org/10.1016/j.tecto.2018.10.033.

Storti, F., Balsamo, F., Mozafari, M., Koopman, A., Swennen, R., and Taberner, C., 2018, Syn-contractional overprinting between extension and shortening along the Montagna dei Fiori fault during Plio-Pleistocene antiformal stacking at the central Apennines thrust wedge toe: Tectonics, v. 37, p. 3690–3720, https://doi.org/10.1029/2018TC005072.

Tavani, S., 2012, Plate-kinematics in the Cantabrian domain of the Pyrenean orogen: Solid Earth, v. 3, p. 265–292, https://doi.org/10.5194/se-3-265-2012.

Tondi, E., 2000, Geological analysis and seismic hazard in the Central Apennines: Journal of Geodynamics, v. 29, p. 517–534, https://doi.org/10.1016/S0264-3707(99)00048-4.

Tondi, E., and Cello, G., 2003, Spatiotemporal evolution of the Central Apennines fault system (Italy): Journal of Geodynamics, v. 36, no. 1–2, p. 113–128, https://doi.org/10.1016/S0264-3707(03)00043-7.

Tondi, E., Chiaraluce, L., and Roberts, G., 2009, Ten years after the Umbria-Marche earthquake: Tectonophysics, v. 476, no. 1–2, https://doi.org/10.1016/j.tecto.2009.06.004.

Torabi, A., Alaei, B., and Libak, A., 2019, Normal fault 3D geometry and displacement revisited: Insights from faults in the Norwegian Barents Sea: Marine and Petroleum Geology, v. 99, p. 135–155, https://doi.org/10.1016/j.marpetgeo.2018.09.032.

Tung, S., and Masterlark, T., 2018, Resolving source geometry of the 24 August 2016 Amatrice, central Italy, earthquake from InSAR data and 3D finite-element modeling: Bulletin of the Seismological Society of America, v. 108, no. 2, p. 553–572, https://doi.org/10.1785/0120170139.

Valoroso, L., Waldhauser, F., Di Stefano, R., Schaff, D., Chiaraluce, L., and Piccinini, D., 2013, Radiography of a normal fault system by 64,000 high-precision earthquake locations: The 2009 L′Aquila (central Italy) case study: Journal of Geophysical Research. Solid Earth, v. 118, no. 3, p. 1156–1176, https://doi.org/10.1002/jgrb.50130.

Villani F., Civico, R., Pucci, S., Pizzimenti, L., Nappi, R., De Martini, P.M., and the Open EMERGEO Working Group, 2018, A database of the coseismic effects following the 30 October 2016 Norcia earthquake in Central Italy: Science Data, v. 5, no. 180049, https://doi.org/10.1038/sdata.2018.49.

Villemin, T., Angelier, J., and Sunwoo, C., 1995, Fractal distribution of fault length and offsets: Implications for brittle deformation evaluation—Lorraine Coal Basin, in Barton, C.C., and La Pointe, P.R., eds., Fractals in the earth sciences: New York, Plenum Press, p. 205–226.

Waldhauser, F., and Ellsworth, W., 2000, A Double-Difference Earthquake Location Algorithm: Method and Application to the Northern Hayward Fault, California: Bulletin of the Seismological Society of America, v. 90, no. 6, p. 1353–1368, https://doi.org/10.1785/0120000006.

Walsh, J.J., and Watterson, J., 1991, Geometric and kinematic coherence and scale effects in normal fault systems, in Roberts, A.M., Yeilding, G., and Freeman, B., eds., The Geometry of Normal Faults: Geological Society of London, Special Publications, v. 56, p. 193–203, https://doi.org/10.1144/GSL.SP.1991.056.01.13.

Walsh, J.J., and Watterson, J., 1988, Analysis of the relationship between displacements and dimensions of faults: Journal of Structural Geology, v. 10, p. 239–247, https://doi.org/10.1016/0191-8141(88)90057-0.

Walsh, J.J., Childs, C., and Nicol, A., 2002, An alternative model for the growth of faults: Journal of Structural Geology, v. 24, no. 11, p. 1669–1675, https://doi.org/10.1016/S0191-8141(01)00165-1.

Walters, R.J., Gregory, L.C., Wedmored, L.N.J., Craig, T.J., McCaffrey, K., Wilkinson, M., Chene, J., Lie, Z., Elliott, J.R., Goodall, H., Iezzi, F., Livio, F., Michetti, A.M., Roberts, G., and Vittori, E., 2018, Dual control of fault intersections on stop-start rupture in the 2016 Central Italy seismic sequence: Earth and Planetary Science Letters, v. 500, p. 1–14, https://doi.org/10.1016/j.epsl.2018.07.043.

Wedmore, L.N.J., Faure Walker, J.P., Roberts, G.P., Sammonds, P.R., McCaffrey, K.J.W., and Cowie, P.A., 2017, A 667 year record of coseismic and interseismic Coulomb stress changes in central Italy reveals the role of fault interaction in controlling irregular earthquake recurrence intervals: Journal of Geophysical Research. Solid Earth, v. 122, https://doi.org/10.1002/2017JB014054.

Willemse, E.J.M., Pollard, D.D., and Aydin, A., 1996, Three-dimensional analyses of slip distributions on normal fault arrays with consequences for fault scaling: Journal of Structural Geology, v. 18, p. 295–309, https://doi.org/10.1016/S0191-8141(96)80051-4.

Wilkins, J.S., and Gross, R.M., 2002, Normal fault growth in layered rocks at Split Mountain, Utah: Influence of mechanical stratigraphy on dip linkage, fault restriction and fault scaling: Journal of Structural Geology, v. 24, no. 9, p. 1413–1429, https://doi.org/10.1016/S0191-8141(01)00154-7.

Withjack, M.O., Schlische, R.W., and Olsen, P.E., 2010, Development of the passive margin of eastern North America: Mesozoic rifting, igneous activity, and drifting, in Bally, A.W., and Roberts, D.G., eds., Phanerozoic Regional Geology of the World: Elsevier, New York, USA, v. 1.

Zoback, M., and Gorelick, S., 2012, Earthquake triggering and large-scale geologic storage of carbon dioxide: Proceedings of the National Academy of Sciences of the United States of America, v. 109, p. 10164–10168, https://doi.org/10.1073/pnas.1202473109.